Downloaded from orbit.dtu.dk on: Apr 25, 2024

DTU Library

Wind farm models and control strategies

Sørensen, Poul Ejnar; Hansen, Anca Daniela; Iov, F.; Blaabjerg, F.; Donovan, M.H.

Publication date:
2005

Document Version
Publisher's PDF, also known as Version of record

Link back to DTU Orbit

Citation (APA):
Sørensen, P. E., Hansen, A. D., Iov, F., Blaabjerg, F., & Donovan, M. H. (2005). *Wind farm models and control strategies*. Denmark. Forskningscenter Risoe. Risoe-R No. 1464(EN)

General rights
Copyright and moral rights for the publications made accessible in the public portal are retained by the authors and/or other copyright owners and it is a condition of accessing publications that users recognise and abide by the legal requirements associated with these rights.

- Users may download and print one copy of any publication from the public portal for the purpose of private study or research.
- You may not further distribute the material or use it for any profit-making activity or commercial gain
- You may freely distribute the URL identifying the publication in the public portal

If you believe that this document breaches copyright please contact us providing details, and we will remove access to the work immediately and investigate your claim.

Risø-R-1464(EN)

Wind farm models and control strategies

Poul Sørensen, Anca D. Hansen, Florin Iov, Frede Blaabjerg
and Martin H. Donovan

Risø National Laboratory
Roskilde
Denmark
August 2005

Author: Poul Sørensen, Anca D. Hansen, Florin Iov, Frede Blaabjerg and Martin H. Donovan
Title: Wind farm models and control strategies
Department: Wind Energy Department

Risø-R-1464(EN)
August 2005

Abstract (max. 2000 char.):

This report describes models and control strategies for 3 different concepts of wind farms. Initially, the potential in improvement of grid integration, structural loads and energy production is investigated in a survey of opportunities. Then simulation models are described, including wind turbine models for a fixed speed wind turbine with active stall control and a variable speed wind turbine with doubly-fed induction generator. After that, the 3 wind farm concepts and control strategies are described. The 3 concepts are AC connected doubly fed turbines, AC connected active stall turbines and DC connected active stall turbines. Finally, some simulation examples and conclusions are presented.

ISSN 0106-2840
ISBN 87-550-3322-9 (Internet)

Contract no.:

Group's own reg. no.:
1115030-1

Sponsorship:
Elkraft System PSO (FU 2102)

Cover :

Pages: 63
Tables: 4
References: 33

Risø National Laboratory
Information Service Department
P.O.Box 49
DK-4000 Roskilde
Denmark
Telephone +45 46774004
bibl@risoe.dk
Fax +45 46774013
www.risoe.dk

Contents

Preface

This report describes results of the project titled “Control of wind power installations”. The project was funded by the Danish TSO, Elkraft System as PSO project FU 2102, and it was carried out in cooperation between Risø National Laboratory, Technical University of Denmark, Aalborg University and Energy E2.

1 Introduction

The wind energy industry has developed rapidly through the last 20-30 years. The factories have developed from small workshops to mature industry, and technically the wind turbines have increased in size, the costs have been reduced, and the controllability developed. This places modern wind energy as a serious and competitive alternative to other energy sources.

The development has been concentrated on wind turbines for electrical power production, i.e. grid connected wind turbines. Grid connected wind turbines are a part of a power system, with which they interact. On one hand, the power system and its quality has an influence on the wind turbines performance, lifetime and safety, and on the other hand, the quality and the reliability of the wind turbine power will influence the power system quality, stability and reliability. Therefore, the integration of wind power into the power systems has become an important issue in development and research of wind power.

The scope of the present report is wind farm control, which involves the control on wind turbine level as well as the overall control on the wind farm level. Historically, the automatic control of wind power installations has been implemented in the individual wind turbines. Remote control and wind farm monitoring systems have been developed in an early stage, but the main aim has been to monitor the wind turbines and enable remote manual control such as shut down, start up etc. However, the recent development of large (typically offshore) wind farms has initiated the development of advanced, automatic wind farm controllers. The large Danish offshore wind farms in Horns Rev and Nysted are significant step in this development.

Traditionally, the main aim of the wind turbine control is to ensure that the wind turbine is able to produce energy at the lowest possible cost, i.e. at minimum price per kWh. Normally, this means that the control should aim at maximum possible power production, limited only upwards to the rated power of the turbine. Another important control aim, which also reduces the price per kWh, is to reduce the structural loads on the mechanical components, which makes it possible to reduce the costs of the mechanical components. Finally, it is a control aim to improve the integration of the wind turbines in the power system, in order to secure quality, stability and reliability, and to reduce the required grid connection costs.

The main aim of the advanced offshore wind farm controllers has been to meet grid integration challenges. The development of wind power from smaller distributed installations to large wind farms has introduced new aspects of the influence of the wind power on the power systems. With limited, distributed installations, the main grid integration concern has been the influence of the power quality of the wind turbines on the voltage quality in the local grid. However, large wind power installations will also influence more system related issues such as power and frequency control, reactive power and voltage control on the transmission system level, and the reliability and stability of the power system.

2 Survey of opportunities

The intension of the present work is to develop and simulate wind farm controllers, which mainly aim at improving the power system integration, but keeps the influence on structural loads and energy production in mind. The intension was also to use available data from the wind turbine controllers in wind speed predictions, and use these predictions to improve the control.

In this chapter, we will look at the possible control improvements, and - when possible - quantify possible benefits of such improvements. First, we will look into which wind speed predictions we can make based on typically available data from wind turbine controllers. Then we will discuss the influence of the control on grid integration, structural loads and energy production, with focus on how the control could be improved in these aspects based on predictions.

2.1 Prediction

A wind farm controller has access to extensive information from the controllers in the individual wind turbines. This information could probably be in many ways by the wind farm controller, but here we will focus on the possibility to use the information to predict the wind speed at individual wind turbines, since the wind speed variation in size and direction is considered the main uncertainty.

Wind speed variations are caused by turbulence, which has a stochastic nature. Still, there is a certain structure in the wind, which makes it possible to make a prediction of the future wind speed, which is better than the so-called persistence, i.e. to provide a better guess on the future wind speed than being equal to the present wind speed.

A very significant contribution to the structure of the turbulence is indicated by Taylor's frozen turbulence hypothesis [1]. Basically, this hypothesis states that the turbulence as "space series", which are moved downwind with the mean wind speed U_0 as illustrated in Figure 1.

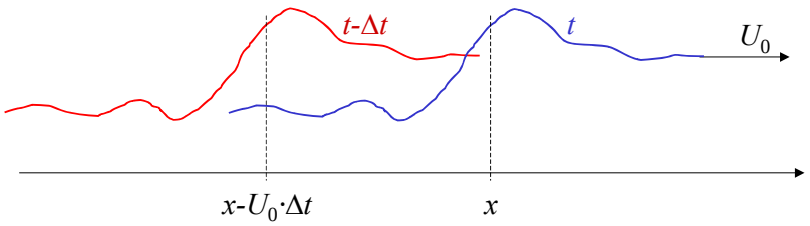

Figure 1. Taylor's frozen turbulence hypothesis.

Thus, the wind speed $U(x,t+\Delta t)$ at position x and time $t+\Delta t$ can be predicted as the $U_0 \cdot \Delta t$ meters upwind wind speed according to

$$U(x,t+\Delta t) \cong U(x-U_0 \cdot \Delta t, t) \qquad (1)$$

However, this Taylor hypothesis is only an approximation, which is most accurate for large variations and small distances. Because new turbulence is generated continuously, the actual structure of the turbulence changes as it moves in the wind direction, and this is particularly important for the smaller variations and the larger distances.

In a wind farm, it could be advantageous to utilise Taylor's frozen turbulence hypothesis to predict the wind speed at the wind turbines. The wind farm controller will have

information about the current wind speeds in at all the wind turbines, and probably also at one or more meteorological masts. Thus many of the wind turbines could take advantage of the “upwind information”.

Table 1 shows the delay time Δt for selected wind speeds and distances relevant in wind farms. Typical distances for large wind farms between wind turbines will be above 300 m. Thus, depending on wind farm layout, wind speed and wind direction, it could be possible to predict the wind speed 15-200 s ahead for most of the wind turbines.

	5 m/s	10 m/s	20 m/s
300 m	60 s	30 s	15 s
500 m	100 s	50 s	25 s
1000 m	200 s	100 s	50 s

Table 1. Delay time corresponding to different mean wind speeds (in columns) and different distances (in rows)

A wind speed prediction tool has been developed by Nielsen et. al. [2]. The model is fitted to a set of wind speed time series measured on Risøs test station for large wind turbines in Høvsøre. The layout of the test station is shown in Figure 2. Wind speed measurements in 80 m height in the 5 met masts have been used, and time series with mean wind directions 180 – 190 degrees have been selected to ensure that the wind seen from one mast is downwind to the wind speed seen from another mast.

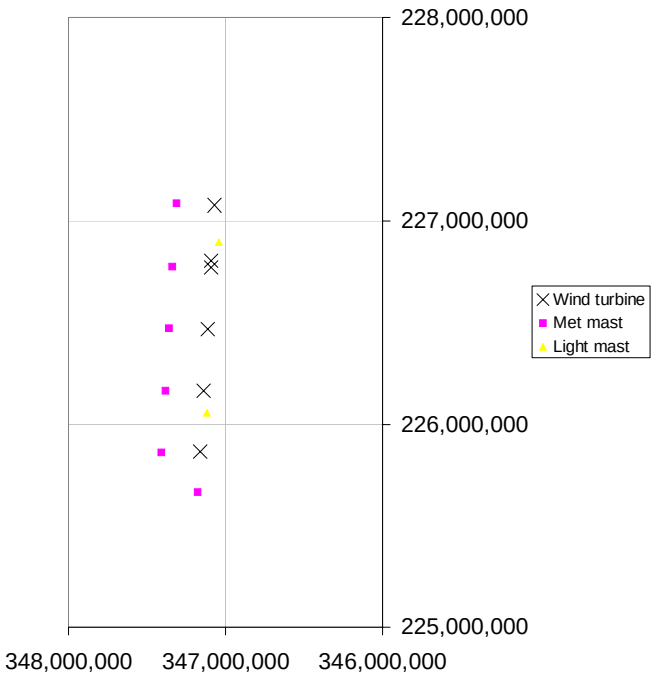

Figure 2. Layout of Høvsøre test station for large wind turbines

An important conclusion of the prediction study was that for pairs of masts with two or three mast in between, the relation between the wind speed series is weak. Even for neighbouring masts, which are placed 300 m from each other, the Mean Absolute Error (MAE) range from just above 0m/s to 0.8m/s, where MAE = 0.8m/s occur for a series with an average wind speed of 19m/s.

This means that for 600 m and above, the relation is weak. Thus it can be concluded that the estimation based on Taylor's frozen turbulence hypothesis is relatively uncertain for typical distances in most large wind farms. This has been taken into account considering the perspective in using the predictions in wind farm controllers. Another issue, which makes the prediction even more uncertain is that the correlation is even weaker when the wind is not directed along a row of wind turbines as it has been in the selected time series. Finally, the wake from wind turbines has not been included in the present modelling and MAE calculation cases. Thus, the "best cases" have been analysed, a certain correlation has been found but the estimates are still relatively uncertain.

2.2 Grid integration

The main task of the wind farm controller is to make the wind farm operate more like a power plant, and ultimately enable the wind farms to replace conventional power plants. The benefit of such functionalities is most obvious in situations with high wind speed, high heat demand and low electricity demand. In such situations, the bound production from wind turbines and local combined heat and power plants is very high, but since the demand is low, the excessive power must be exported.

In the west Danish system, it now often happens that the bound production exceeds the demand. These situations also cause the electricity prices to decrease. Still, in these situations, a number of conventional plants are kept in operation at low production, with reduced efficiency, simply to ensure the control and stability of the system. If the wind farms are provided with controllability similar to the large power plants, it is most likely possible to save the total system operational costs by shutting down one or more conventional plants.

Power and frequency control

The generated power in the power system must be in balance with the demand from loads and losses in the system. A generator driven by a steam turbine can be represented as a large rotating mass with two opposing torques acting on the rotation [3]. Whenever there is a surplus of generation in the power system, this will cause the synchronous generator to accelerate, and consequently the frequency in the system will increase. Likewise, if there is a deficit of generation, the generator will decelerate, and consequently the grid frequency will decrease.

Therefore, the power balance in the system can be obtained by controlling the rotational speed of the generators. This task is performed by the speed governors of the turbines driving the generators (the prime movers). Conventional large power plants use synchronous generators, and in that case the speed of the generators is proportional to the power system frequency.

According to e.g. [3] and [4], the frequency control of conventional power plants use droop control as illustrated with the solid line in Figure 3 to maintain the balance between generation and demand. The governor automatically controls the generation to follow the line with a specific droop R (here 4%). This control is relatively fast, and is often denoted primary control.

Depending on the type and design of prime mover and governor, the idealised characteristics in Figure 3 is often more complex. As an example, according to Lindahl [5], governor dead-band, lowpass filtering and non-linearities in generating units have a significant influence on the primary response in the Nordic system.

The dashed lines in Figure 3 show alternative governor settings, which can be set manually or by Automatic Generation Control (AGC). This change in governor settings is slower than the primary control, and is often denoted secondary control. The secondary control is used by the dispatch centre to control the distribution of the generation between the plants in the system, mainly in order to minimise the total generation costs.

When the governor settings are changed as indicated in Figure 3, it should preferably not change instantaneously. Sudden changes in generation could cause unnecessary frequency changes and other stability problems. Also the mechanical stressing and the dynamic limitations of conventional power plants restricts the possible and desired rate of change of the setpoint. Therefore, it is common to specify power ramp rates used in the secondary control with power plants.

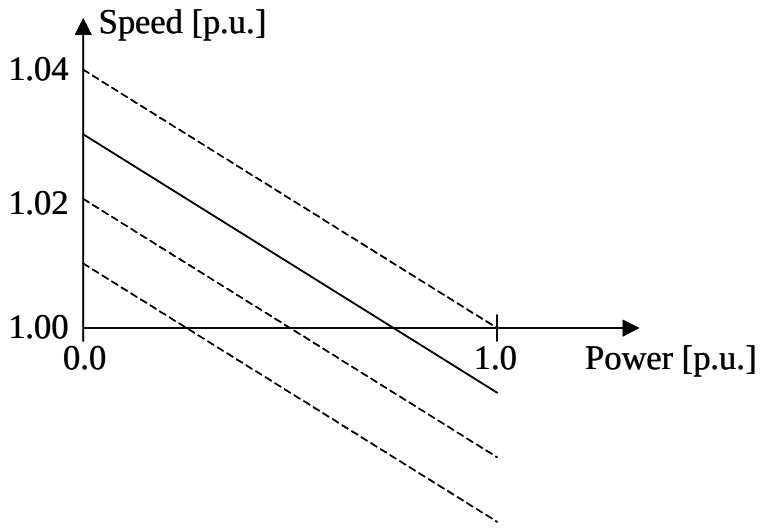

Figure 3. Droop characteristics for conventional power plant. The droop R = 0.04 (or 4%).

Support for primary control is required in Danish Transmission system operator's new regulations for grid connection of wind turbines and wind farms to the grid below 100 kV [6], [7], and additional support to secondary control is required for large wind farms connected to voltages above 100 kV [7]. To support primary control, the operator must be able to specify droop as well as dead-band, whereas e.g. balance and delta control with ramp rate limitation is required to support the secondary frequency control.

Wind turbines in general and large wind farms in particular are able to participate in the primary as well as the secondary frequency control. However, primary and secondary frequency control tasks for the wind farm would normally mean loss of wind power generation, obviously without any fuel saving in the wind farm. Another issue concerning frequency impact is the influence on system inertia, and concerning that area wind turbines can contribute without significant losses of wind power generation.

The inertia of the directly AC connected rotating machines including the inertia of power plant generators and turbines is essential for the frequency control. When an unbalance between generation and demand occurs, the inertia limits the rate of change of the

frequency. The generators in the system rotate synchronously with the angular frequency ω, and the equation of motion of each machine with inertia I is given by (2).

$$I\dot{\omega} = T_m - T_g \tag{2}$$

Here, T_m is the mechanical torque from the turbine on the generator shaft, whereas T_g is the generator torque caused by the electrical load on the machine. If there is surplus generation, i.e. T_m - T_g > 0, then the inertia starts accelerating. However, if the inertia is very large, this acceleration becomes slow. The acceleration, which is the rate of change of the speed, is very important for the frequency control because slower changes in the frequency ensures that the primary control gets more time to respond to the changes in the frequency.

Holdsworth et.al. [8] have studied the impact of fixed speed and variable speed wind turbines on the inertia in the power system. It was observed that standard fixed speed wind turbines with directly connected generators contribute to the inertia of the power system with the inertias of the generator and the wind turbine rotor, whereas standard variable speed wind turbines control power independently on the grid, and thus decouple the generator torque from the grid frequency. This gives variable speed wind turbines virtually zero inertia seen from the power system. However, since the generator torque is controlled directly in variable speed wind turbines, the control system of a wind farm or a wind turbine controller for variable speed wind turbines can be programmed to provide virtual power system inertia. This only requires a reliable and fast measurement of the rate of change of the grid frequency.

A virtual inertia control for a variable speed wind turbine will use a virtual inertia parameter as input. In principle, any size of the virtual inertia can be specified. If the virtual inertia I_{virt} is specified to be equal to the actual inertia I_{act} of the generator and wind turbine rotor, then the wind turbine generator speed ω_{gen} would change proportionally to the grid frequency f. Alternatively, if the virtual inertia is specified to the double of the actual, then changes in grid frequency would cause the double change in wind turbine generator speed. This can also be expressed according to (3).

$$\Delta\omega_{gen} = \frac{I_{virt}}{I_{act}} \cdot \frac{\Delta f}{f} \cdot \omega_{gen} \tag{3}$$

So in principle we can specify a very high virtual inertia, but that would cause the wind turbine to loose much speed for smaller changes in the grid frequency. The problem is then that when the wind turbine looses speed, the aerodynamic rotor would not produce the same mechanical torque, and consequently the turbine could loose further speed and thus become unstable. Therefore, if virtual inertia is implemented in the controllers, it is an issue to determine how large the virtual inertia can be specified without loosing the stability.

The issue of inertia is particularly important for high wind power penetration levels in a synchronous system. As long as the west Danish system is connected synchronously to the UCTE system, the inertia of the wind turbines is probably not an issue. But if the system should be able to continue operation when the connection to the UCTE system is lost, then a certain sum of inertia would be necessary to keep the frequency stable. For the same reason, there is a particular focus on the influence of different wind turbine types on the power system inertia in the Irish island system [9].

It has been considered if the possible wind speed forecasting based on wind farm controller information can be useful for the power and frequency control. The aim could be to use the predictions to smooth the power produced by the wind farm. Measurements in the connection point of the 160 MW Horns Rev wind farm have shown that the power can change by up to 100 MW in 15-20 minutes – Akhmatov et. al. [10]– because of weather conditions, and this is a problem especially if a second large offshore wind farm is built close to the existing. Akhmatov et. al. have shown that ramp rate limitation and area controller operation can reduce the fluctuations considerably. A 10-30 minute accurate forecast of wind speeds, which is able to predict large wind speed changes in the whole wind farm area, could probably be used to improve the control further. However, such a prediction cannot be obtained based on the measurements available in the wind farm controller, since it would require wind measurements up to 10-40 km upwind from the wind farm to observe the large changes 30 minutes before they reach the wind farm.

Reactive power and voltage control

Reactive power control and voltage control are strongly related in power system control. This is because there is a very strong coupling between the reactive power flow and the voltage differences in the grid. According to e.g. [4], transmission of active power P and reactive power Q through a transmission line with serial line resistance R and serial line reactance X, will result in the voltage difference ΔV which is by the first approximation

$$\Delta V \cong \frac{R \cdot P + X \cdot Q}{V} \tag{4}$$

For transmission system networks, where the large wind farms have to be connected, it is normally a reasonable assumption that $X >> R$. In that case, it is seen from (4) that the reactive power Q and the voltage difference ΔV are approximately proportional, which means that the reactive power is ideal to control voltage.

In distribution networks where smaller wind power installations can be connected, the size of R is often comparable in size to X, and for ends of long lines, R may even be larger than X. In that case, the voltage dependence of the active power should also be taken into account in assessment of the influence on the local voltage. However, if the active power balance is used by the system frequency control as described above, the voltage can only be controlled by reactive power.

If the voltage is controlled in both ends of the transmission line, then the reactive power flow Q is determined by the difference ΔV in the voltage setpoints, and it is easy to see from (4) that if this voltage difference is too big, and at the same time the transmission reactance is small, then a very large reactive power flow is the result. This flow will cause unnecessary losses, and also the voltage control may become unstable.

This is also an issue considering voltage regulation of a wind farm. If all wind turbines in a wind farm are trying to participate independently in the voltage control by changing its own reactive power to control voltage on its own terminals, this may cause unnecessarily large flows of reactive power between the turbines. Instead, the voltage control should be monitored by a wind farm controller, which controls the voltage in the wind farm connection point by changing the reactive power setpoints of the individual wind turbines.

Thus, it is necessary to distinguish between reactive power or power factor control on one side, and direct voltage control on the other side. Conventional large power plants

control the voltage in the connection point, while single wind turbines and other distributed generators normally control the reactive power or the power factor.

Large wind farms connected to the transmission system must also be able to control the voltage directly, if they should be able to replace conventional power plants. In the present project, both reactive power control and direct voltage control is developed.

2.3 Structural loads

The loads on the mechanical structure of the wind turbine have been a main driver for development of pitch controlled wind turbines from fixed speed turbines to variable speed turbines.

Not only the hardware, but also the selected control strategy of the wind turbine will influence the structural loads and consequently component lifetime of the wind turbine. As part of the present project, Thomsen [11] carried out an investigation of fatigue loads for a wind turbine operating at 100% and at 50% power. The idea of this investigation was to provide input for optimizing the trade-off between power production and life time consumption of a wind turbine.

The investigation of the fatigue loads used a wind turbine modelled in Risøs HAWC software [12] with data representative for modern commercial MW turbines, in terms of aerodynamics, structural dynamics and control design. A reference design load basis was established for the reference turbine. This was based on IEC61400-1 class IA. For a number of load sensors, fatigue analyses were carried out, and the contribution of each load case to the total fatigue damage was mapped.

It was the general conclusion that the load cases representing power production during normal operation contribute significantly to the total fatigue damage for most load sensors, which enables the possibility of optimizing the trade-off between power production and life time consumption.

Two different operational strategies for the turbine were considered. Both strategies are with reduced power (to a level of 50%), but they differ in the way the power reduction is reached. In one case, the power is reduced by a change in pitch angle, and in the other case, the power is reduced by a reduction in rotational speed. In order to avoid problems with stall, the latter strategy also involves a minor change in pitch angles at low wind speeds.

The fatigue loads for the two modified strategies were very different. For the strategy with reduced power by pitch angle change, no significant change in fatigue loads were obtained - compared with the reference turbine (100% power). However, for the strategy with reduced power by a reduction in rotational speed, the rotor fatigue loads were reduced by a factor of 25% to 50% - compared with the reference turbine. The fatigue load reduction for the tower loads were, however, less significant.

This result is important not only for investigation of the trade-off between power production and life time consumption, but also for the way that the power control for grid support in section 2.2 should be implemented. Taking only the grid integration issue into account, it would be beneficial to reduce the wind turbine power by pitching the blades and keeping the rotational speed to a maximum. That way, the reserves would be available with very short response time, requiring only to pitch the blades. Also, energy can be stored if the rotational speed is higher than the optimal for the given wind speed.

However, the fatigue investigations show that such an operational strategy would increase the lifetime consumption of the wind turbine components, especially the blades.

It has been considered if the predictions described in section 2.1 can be used to reduce the structural loads. However, studies of improvement of control strategies to reduce structural loads indicate that the control system would need information about the spatial variations of the wind speed over the wind turbine rotor area rather than the expected average rotor wind speed 10-60 seconds ahead. For instance, Larsen et. al. [13] have studied cyclic pitch of the individual blades, which can reduce the structural loads. Thus, it is not likely that the predicted wind speeds can be used to reduce structural loads.

2.4 Energy production

Another area where the predictions could be used is to increase the energy production of the wind turbines. For wind farms with fixed speed wind turbines with a slow active stall control of the blades, it might be possible to increase the production a little or to reduce the pitching activity if the wind speed can be predicted. However, the blades can normally be pitched relatively fast to the optimal position.

Simulations with variable speed [14] show that the generator speed response to wind speed changes is relatively slow, apparently with time constants above 10 seconds in the low wind speed range. American research results from the NREL variable-speed test bed [15] showed that there is a substantial gap between the idealised power production and the actual power production of a variable speed wind turbine in the wind speed region where the rotational speed of the wind turbine is controlled to provide maximum power. It was also stated that "This gap is about 10% and is caused primarily by the inability of the rotor to accelerate and decelerate quickly enough to keep instantaneous λ perfectly constant at the desired value". Later [16] the conclusion was moderated to "that a very common 5% error in the optimal tip-speed-ratio λ* alone can cause an energy loss of around 1% - 3% in region 2." "Region 2" is the low to medium wind speed range where the control strategy is to keep the rotational speed proportional to the wind speed in order to produce maximum power, i.e. to keep the tip-speed-ratio λ to a constant, optimal value λ_{opt}. λ is defined by the rotational speed ω_{rot}, wind turbine radius R and wind speed u according to (5)

$$\lambda = \frac{\omega_{WTR} \cdot R}{u} \tag{5}$$

Thus, the American research results indicated that standard variable speed control causes a significant spill of power, which can be retrieved by an improved control strategy, e.g. based on wind speed prediction. On this background, the possible energy production is quantified in the following based on simulations. The advantage of using simulations is that a more accurate estimate of the power production gap caused by the slow speed control can be obtained.

Figure 4 shows 600 seconds simulation with the pitch controlled double fed (i.e. variable speed) wind turbine model described in chapter 4.2. The mean wind speed 6 m/s has been selected, to ensure "region 2" operation, i.e. power optimisation. If the wind speed gets outside this region, the rotational speed will be controlled to constant. 20 % turbulence intensity has been selected as a "worst case" with maximum turbulence, which is expected to give maximum deviation from the ideal operation with optimal tip-speed-ratio.

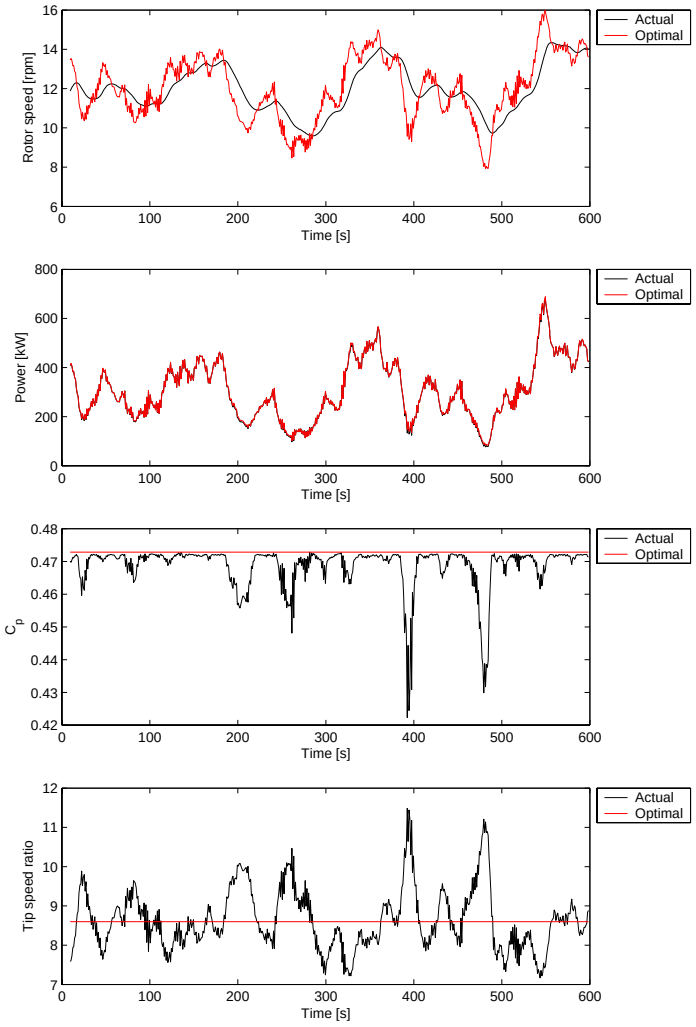

Figure 4. Simulated ("actual") and optimal operation of variable speed (double-fed) wind turbine. Wind speed input is simulated using 6 m/s mean value and 20% turbulence intensity.

From the first graph it is seen how the actual rotational speed is smoother and delayed compared to the optimal speed. The optimal speed is calculated as ω_{rot} using (5) with $\lambda = \lambda_{opt}$. The second graph shows the actual (simulated) power compared to the optimal power P_{opt} calculated according to

$$P_{opt} = \frac{1}{2} \cdot \rho \cdot A \cdot u^3 \cdot C_p\left(\lambda_{opt}\right) \tag{6}$$

It is seen that the actual power is very close to the optimal, since it is very difficult to distinguish the two curves in the second graph. The third graph shows the simulated (actual) power coefficient C_p and the optimal value $C_p(\lambda_{opt})$. This graph reveals significant dips in C_p corresponding to power production significantly (around t=390 s more than 10 %) below optimum. However, it should be noted that the dips are very short in duration and not so many.

The fourth graph shows the corresponding actual and optimal tip speed ratio. It is seen that the tip speed ratio (and consequently the rotational speed) is generally too high when the power (and consequently wind speed) decreases, while the rotational speed is too low when the wind speed increases. This is as expected, because the controller delays the response in rotational speed.

In Figure 5, a similar simulation is performed, but this time a more realistic wind speed time series is used. The wind speed is measured in 80 m height on Risøs test station for larger wind turbines in Høvsøre 24 July 2003, 22:50. However, the measured wind speed has been modified using the rotor wind model – see section 4.2 below – to provide an equivalent wind speed as seen from the rotating blades.

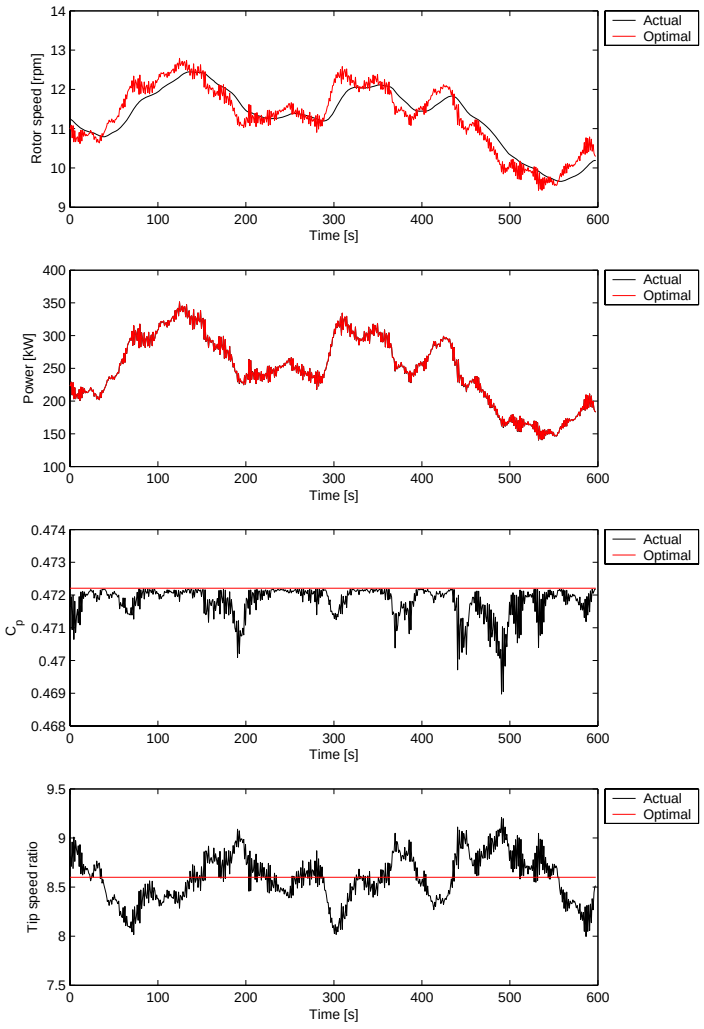

Figure 5. Simulated ("actual") and optimal operation of variable speed (double-fed) wind turbine. Simulation is based on Høvsøre wind speed measurement 2003-07-24 22:50 with 5.5 m/s mean wind speed and 8.7% turbulence intensity.

The results of the two simulations above are shown in Table 2 together with another simulation with Høvsøre measured wind speed. It is seen that while 0.57% power is

spilled in the simulation with 20 % turbulence intensity, the spilled power is only 0.07-0.09% using the measured wind speed time series with less than 9% turbulence intensity. This result suggests that there is not much point in improving the speed control to increase power production, because less the 0.09 % power increase can be obtained even with perfectly fast speed control.

Wind input	$E\{U\}$	$\sigma\{U\}$	$\frac{E\{\lvert\lambda - \lambda_{opt}\rvert\}}{\lambda_{opt}}$	$\frac{E\{P\} - E\{P_{opt}\}}{E\{P_{opt}\}}$
Simulated	6.0 m/s	1.2 m/s	7.4 %	-0.57 %
Høvsøre M5 2003-07-24 22:50	5.5 m/s	0.48 m/s	2.5 %	-0.09 %
Høvsøre M5 2003-07-24 22:40	5.7 m/s	0.36 m/s	2.1 %	-0.07 %

Table 2. Maximum power tracking simulation results, general turbine C_p

This result is surprising, keeping in mind the NREL test bed results with an energy loss of around 1% - 3%. A number of reasons can explain some of the differences:

1. Using both measurements and idealised calculations to quantify the gap in power due to the speed control as NREL has done, several other factors and error sources influence the result.
2. The speed-torque characteristics used in the controller can be wrong, which will cause additional energy losses. We have looked at this issue also, but it seems that the controllers are quite robust to this error.
3. The inertia of the rotor compared to the rated power is important because the time constant of the speed control delay depends on the inertia.
4. The turbulence intensity can be very different for the small wind turbine on the NREL site compared to 80 m height in Høvsøre.
5. The $C_p(\lambda)$ characteristics has a significant influence. The characteristics used in this project correspond to the rotor of a standard 2MW wind turbine, and it has a relatively flat maximum.
6. The use of the rotor wind speed model is important, especially for large rotors

A few more simulations have been performed to quantify the influence of some of these factors. The results are shown in Table 3. First the influence of using the equivalent wind speed is seen, comparing the first and second result in Table 3. It is seen that we simulate that more power is spilled if we use the measured wind speed directly. This is because the equivalent wind speed fluctuates less that the measured, because the rotor filters the wind speed. Especially large wind turbine rotors have a significant filtering effect.

Comparing the first and third result in Table 3 quantifies the influence of the $C_p(\lambda)$ characteristics. As mentioned above, the $C_p(\lambda)$ used in the first result correspond to the rotor of a standard 2MW wind turbine, and it has a relatively flat maximum. In the third result in Table 3, we have used a more steep $C_p(\lambda)$ characteristics, see Figure 6. In this

case, the consequence of a certain deviation from optimal speed is a larger dip in $C_p(\lambda)$ and consequently more spilled power.

Wind input	$\frac{E\{\lambda - \lambda_{opt}\}}{\lambda_{opt}}$	$\frac{E\{P\} - E\{P_{opt}\}}{E\{P_{opt}\}}$
Measured converted to equivalent wind speed	2.5 %	-0.09 %
Directly measured wind speed	3.4 %	-0.16 %
Measured converted to equivalent wind speed, dedicated var-speed C_p	2.5 %	-0.15 %

Table 3. Maximum power tracking simulation results, Høvsøre Mast 5, 2003-07-24 22:50, mean wind speed 5.5 m/s, turbulence intensity 0.087

The variable speed C_p characteristics in Figure 6 is only steeper than the general 2MW turbine characteristics when the tip speed ratio decreases from the optimum value λ_{opt} = 8.6. If the tip speed ratio increases with up to 10 %, the variable speed characteristics are quite similar to the general 2 MW turbine characteristics.

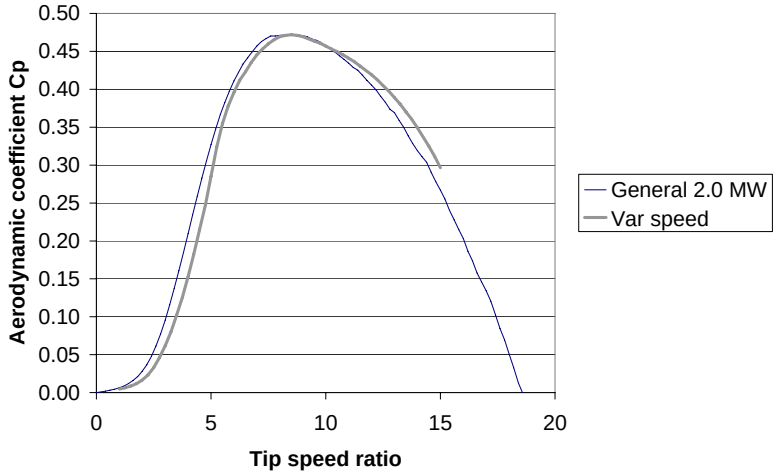

Figure 6. Cp characteristics used for simulations with results in Table 3.

The conclusion of the present simulation results is that there is very little spilled energy, which could be retrieved by an improved variable speed control. This combined with the limited accuracy of a prediction indicates that predictions cannot be used to speed up the speed control and thereby increase power production towards maximum possible.

2.5 Conclusion

Summarising the conclusions above, wind speed predictions based on available information in wind farm controllers have not been found useful to improve wind farm controllers significantly. On this background, the further results have focused on developing simulation models and wind farm controllers which support the grid integration, with special focus on the active power / frequency control and reactive

power / voltage control required in the Danish specifications for grid connection of large wind farms.

3 Functional description of wind power plant

In this chapter, the general functional description of the simulated wind farm controllers is given. The description is focused on the behavior of the wind farm seen from the grid side. The present description is based on the Danish TSOs requirements for grid connection of large wind farms [7]. These specifications are very similar to what has already been implemented in the Horns Rev controller [17].

3.1 Power and frequency control

The Danish TSO requirements involve different types of power control: absolute power limitation, delta limitation, balance control, stop control, ramp limitation, and fast down regulation to support system protection. On top of that, automatic frequency control is required. In the present simulated wind farm controller, balance and delta control is implemented together with a ramp limitation. Also, automatic frequency control has been implemented.

The structure of the controllers is illustrated in Figure 7. The wind farm controller is responsible for providing the power demanded by the operator in the point of common coupling (PCC) of the wind farm. The wind farm controller ensures the required power in PCC by setting the power references in the individual wind turbines. The individual wind turbine controllers then controls the power to the requested reference in the wind turbine connection point. Due to losses in the wind farm grid, the sum of power produced by the wind turbines is higher than the power measured in the wind farm PCC.

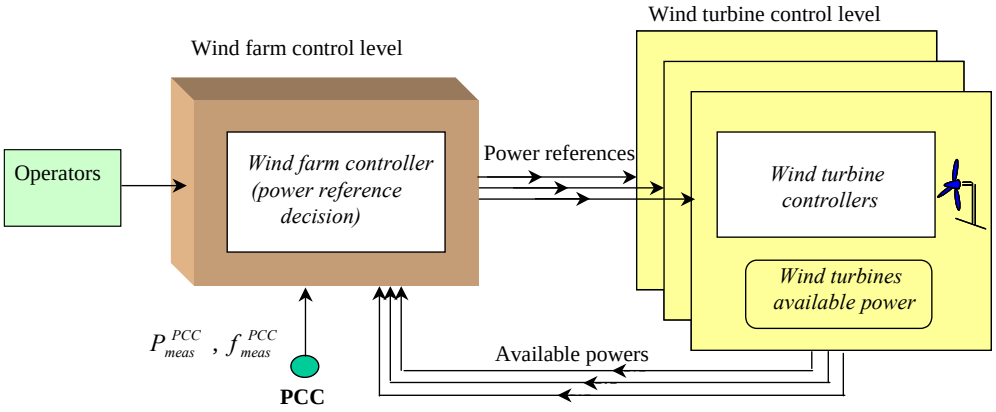

Figure 7. Control structure of wind farm and wind turbine controllers

The wind turbines feed back information to the wind farm controller and the operator on what the available power is. The available power is important because the wind turbines sometime produce less than maximum possible, and if the power reduction is due to TSO requirements e.g. to balance power in the grid, the lost power should be accounted for and therefore quantified as accurate as possible. Also the wind farm controller can benefit from knowledge on the available power as will be seen later.

Figure 8 shows an example of balance control of the output from the wind farm. At time 100s, the power is ordered down to 60 MW. However, the ramp limitation prevents the

power from changing immediately. At time 300s, the power is ordered back to maximum, and again the ramp rate limitation prevents sudden power changes.

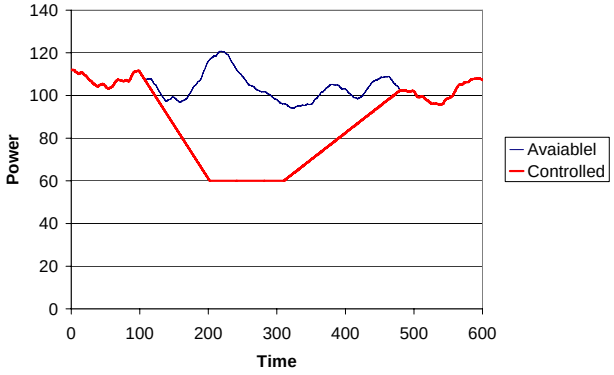

Figure 8. Balance control of wind farm combined with ramp limitation.

Figure 9 shows similar plot for delta control. The advantage of the delta control is that a specified amount (the delta) of reserve power is always available. This can be utilised in automatic primary frequency control.

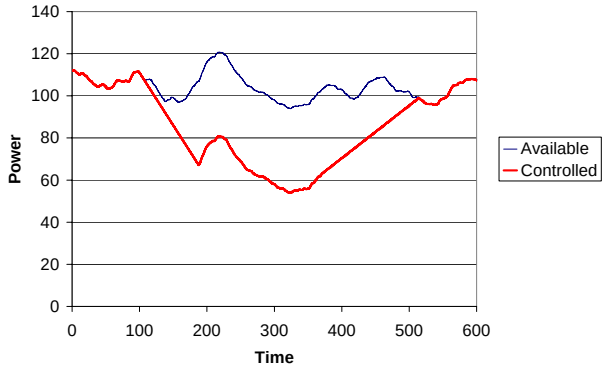

Figure 9. Delta control of wind farm combined with ramp rate limitation.

The primary frequency control includes droop and dead band as shown in *Figure 10*. In normal operation (without activated balance or delta control), the power setpoint P_0 will be equal to the maximum available power P_{max}, and the power – frequency characteristics in *Figure 10* will only have droop for over-frequencies, because there is no reserve power available for under-frequencies.

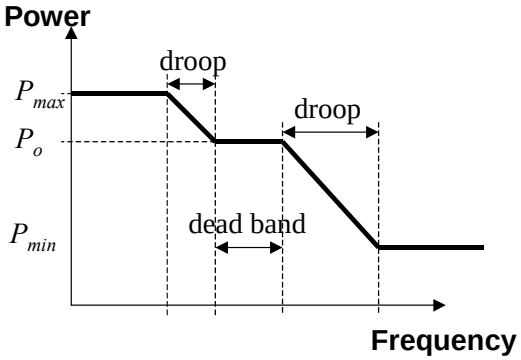

Figure 10. Requirement for automatic frequency control with adjustable droop and dead band.

It is specified in the Danish TSO requirements that the individual wind turbine controllers should change the production depending on the frequency, i.e. according to *Figure 10*. According to Kristoffersen [17], this is also the way frequency control has been implemented in Horns Rev. However, in the present simulations, it has been chosen to implement primary frequency control in the wind farm controller instead of the individual wind turbines. This is because a closed loop power control in the wind farm controller would counteract the attempt of the individual wind turbines to control power depending on frequency, which will damage the frequency control and maybe even make the power control unstable.

It is understood that there were a number of reasons to require the frequency control implemented in the individual wind turbines. The main reasons were:

1. The frequency control response should be as fast as possible. Implementing it in the wind turbines, it would not be slowed down by the communication between the wind farm controller and the wind turbines.
2. It is important that the frequency control and power control is not implemented in the wind farm controller by shutting down some of the wind turbines, but that the wind farm power is reduced by reducing power on all wind turbines and keeping all wind turbines on-line.
3. By requiring control in individual wind turbines, the requirements for single wind turbine installations would be the same as for wind turbines in wind farms.

It is not clear to the authors how the conflict between the frequency control in the individual wind turbines and the wind farm power control is avoided in Horns Rev. It could be met partly if the frequency response is only required on a very short term, i.e. a few seconds, because the wind farm power control is slow. However, a better way to avoid the conflict would be to implement the wind farm power controller as an open loop controller rather than a closed loop controller. This would mean that the sum of power from the individual wind turbines is controlled instead of the actual power though PCC. Assuming that the wind farm controller knows which wind turbines are available, the error would be limited to the losses in the wind farm grid.

As mentioned above, we have chosen to simulate the frequency control implemented centrally in the wind farm controller. Thus, the wind turbine controllers should not respond to the grid frequency but only deliver the reference power, because the wind farm controller has already set the reference power according to the grid frequency. This centralised frequency control seems to be the most robust and consistent solution from a control point of view, because power and frequency are controlled on the same level,

here the wind farm level. Such a wind farm controller will be able to control the power delivered at PCC accurately, and it will automatically compensate for dropouts of individual wind turbines by changing the power from the remaining connected turbines whenever it is possible. It will not have to rely on information from wind turbines if they have been disconnected. If the communication between a certain wind turbine and the wind farm controller is not working, this turbine can still work autonomously, and the wind farm controller will control the remaining wind turbines so that the summed wind farm power delivered in PCC is controlled. Moreover, it is not expected that the frequency control response time will suffer very much from the communication time delay between wind farm controller and wind turbines, because this delay will be very small in future wind farms with modern communication equipment.

3.2 Reactive power and voltage control

According to the Danish TSO requirements, it is required as a minimum that the reactive power from a large wind farm can be controlled to a specific interval, which is close to unity power factor. The exact requirement can be seen in [7]. However, most wind turbines are also able to provide more advanced reactive power control, which can be useful as grid support. Depending on the technology and the electrical design, such wind turbines will normally have some additional capacity for reactive power, although the available reactive power normally depends on the active power as it does for any other generating units in the power system. This dependency is expressed in the PQ diagrams. According to [7], the TSO should have access to the reactive power, and the PQ diagram of the wind farm should be delivered by the owner.

The additional reactive power capacity can either be used to control constant reactive power or constant power factor, or it can be used in automatic voltage control. In the latter case, it is essential, that it is the voltage in the wind farm point of common coupling (PCC) which is controlled, and that this is done on the wind farm controller level. If the wind turbines are individually attempting to control the voltage in the individual connection points, there is a risk of instability and/or unnecessarily high flow of reactive power between the wind turbines.

The possible voltage control in the PCC is of course limited by the limited reactive power available in the wind turbines or from other compensation equipment in the wind farm. For the simulated wind farm controllers presented in this report, we have implementing reactive power / voltage control as a combined droop and deadband control illustrated in Figure 11.

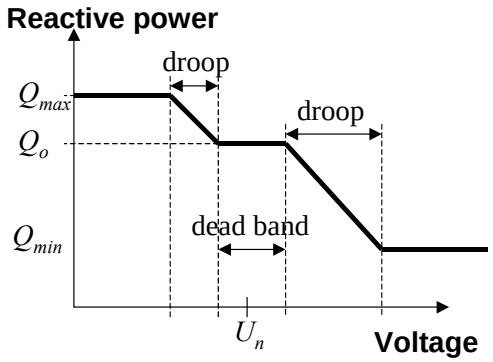

Figure 11. Specified automatic voltage control with adjustable droop and dead band.

4 Simulation models

4.1 Selected wind farm layout

The layout of the wind farm, which is modelled in the present project, has been selected to be very simple. Actually, it would be more correct to denote the layout a cluster rather than a wind farm, but in this report it will be denoted the model wind farm.

The simple layout has been selected because the purpose is to develop new types of controllers and to study how the controllers work in different situations. For that purpose, it is most convenient to reduce the simulation time of the models, which strongly depends on the selected number of wind turbines. On the other hand, the models should include the relevant effects of a wind farm, i.e. a single wind turbine is not sufficient.

The model wind farm layout is shown in Figure 12. The layout is selected as 3 wind turbines on a line, with the same distance and orientation as the measurement masts in Høvsøre. Besides, it is assumed that a measurement mast is available another 307 m down the line.

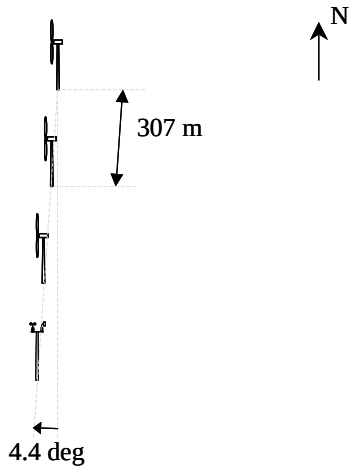

Figure 12.Layout of model wind farm.

The hub height of the wind turbines is selected to 80 m, corresponding to the measurement height in Høvsøre. The rated power of each wind turbines is 2MW, and the same blades are used for active/combi stall controlled wind turbines as well as pitch controlled wind turbines with double fed induction generators.

4.2 Wind turbine models

A simplified block scheme of the wind turbine models is shown in Figure 13. The basic block scheme of the wind turbine consists of a wind model, an aerodynamic model, a transmission system, generator model and a control block model.

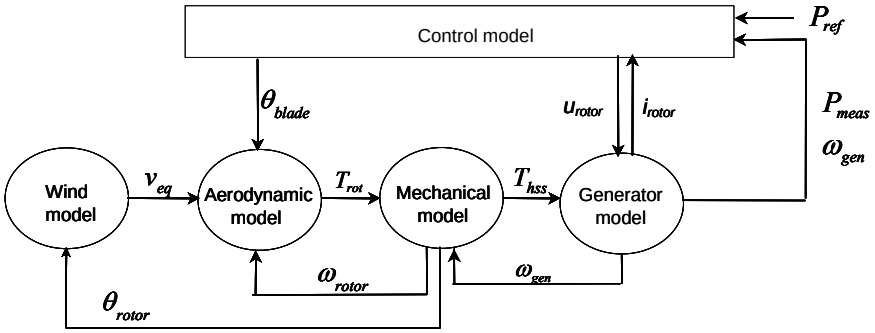

Figure 13. Scheme of wind turbine models.

Wind model

The wind model used is described in detail in [18]. The main advantages of this wind model are the fast computation, reduced memory requirements and the ease of use, either for variable or constant speed models. This wind speed model is very suitable for simultaneous simulation of a large number of wind turbines, making it possible to estimate efficiently the impact of a large wind farm on the power quality.

The structure of the wind model is shown in Figure 14. It provides an equivalent wind speed v_{eq} to the aerodynamic model. The wind model includes two sub-models: a hub wind model and a rotor wind model.

The hub wind model models the fixed-point wind speed at hub height for each wind turbine. In this hub wind model, the park scale coherence is taken into account in the case when a whole wind farm is modelled. The second is the rotor wind model, which includes the averaging effect of the wind speeds over the whole rotor, the rotational sampling effect, and a tower shadow model. The wind shear is not included in the rotor wind model, as it only has a small influence on the power fluctuations.

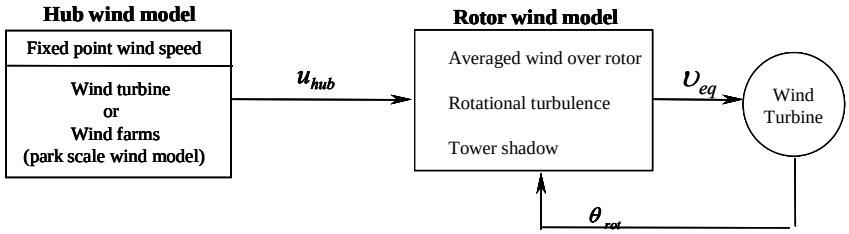

Figure 14: Structure of the wind model.

Notice that the rotor position θ_{rot} is used in the wind model, and the wind model can be used both for variable speed and constant speed wind turbines.

Mechanical model

In the mechanical model, the emphasis is put only on those parts of the dynamic structure of the wind turbine that contribute to the interaction with the grid. Therefore only the drive train is considered in the first place, because this part of the wind turbine has the most significant influence on the power fluctuations. The other parts of the wind turbine structure, e.g. tower and the flap bending modes, are neglected.

The mechanical model is shown in Figure 15. It is essentially a two mass model connected by a flexible low-speed shaft characterized by a stiffness k and a damping c.

The high-speed shaft is assumed stiff. Moreover, an ideal gear with the exchange ratio $1:\eta_{gear}$ is included.

The two masses correspond to the large turbine rotor inertia J_{rot}, representing the blades and hub, and to the small inertia J_{gen} representing the induction generator. The generator inertia is actually included in the generator models in DIgSILENT.

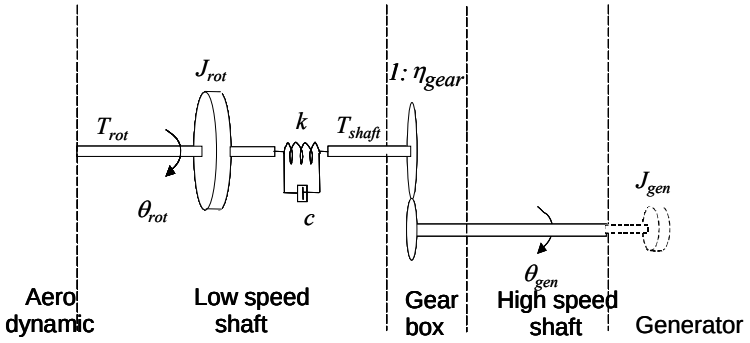

Figure 15: Mechanical model of wind turbine drive train.

Aerodynamic model

The aerodynamic model is based on tables with the aerodynamic power efficiency $C_p(\theta,\lambda)$ or torque coefficient $C_q(\theta,\lambda)$, which depend on the pitch angle θ and on the tip speed ratio λ. This is a quasistatic aerodynamic model which determines the output aerodynamic torque directly from the input wind speed according to:

$$T_{rot} = \frac{P_{rot}}{\omega_{rot}} = \frac{1}{2\ \omega_{rot}}\ \rho\ \pi\ R^2\ \ u^3\ \ C_p(\theta,\ \lambda) \tag{7}$$

or

$$T_{rot} = \frac{1}{2}\ \rho\ \pi\ R^3\ \ u^2\ \ C_q(\theta,\ \lambda) \tag{8}$$

The aerodynamic model can also include a model for dynamic stall as described in Sørensen et.al. [19]. The implemented model for dynamic stall is based on Øye's dynamic stall model [20].

Active/combi stall controlled wind turbines

The layout of the active stall wind turbine is shown in Figure 16. Each wind turbine is connected to a 10 kV busbar. The induction generator, softstarter, the capacitor bank for reactive power compensation and the step-up transformer are all placed in the nacelle, and thus the transformer is considered part of the wind turbine. The control of active and reactive power is based on measured reactive power at the Main Switch Point MSP.

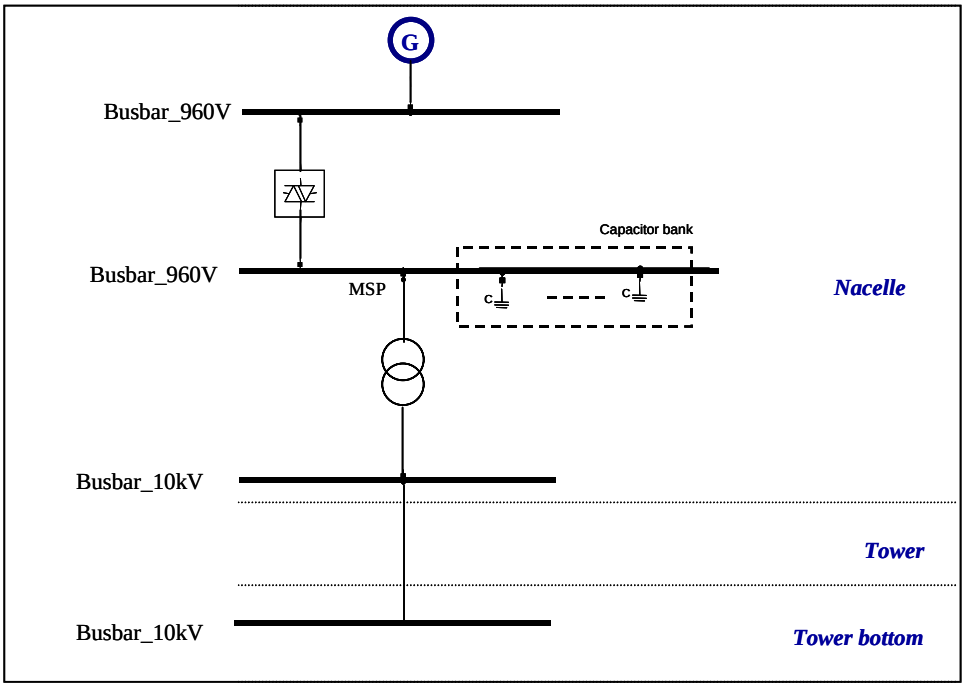

Figure 16: Active stall wind turbine layout including softstarter and capacitor bank.

The wind turbine controller must be able to adjust the wind turbine production to the power reference computed in the wind farm control system, according to the demands imposed by the system operator. In case of normal operation conditions, the wind turbine has to produce maximum power. In power limitation operation mode, the wind turbine has to limit its production to the power reference received from the wind farm controller. The power reference sent by the wind farm controller can be equal to the rated power of the wind turbine or less than that. Figure 17 illustrates the power curves and C_p curves for a 2 MW active stall wind turbine for different imposed power setpoints.

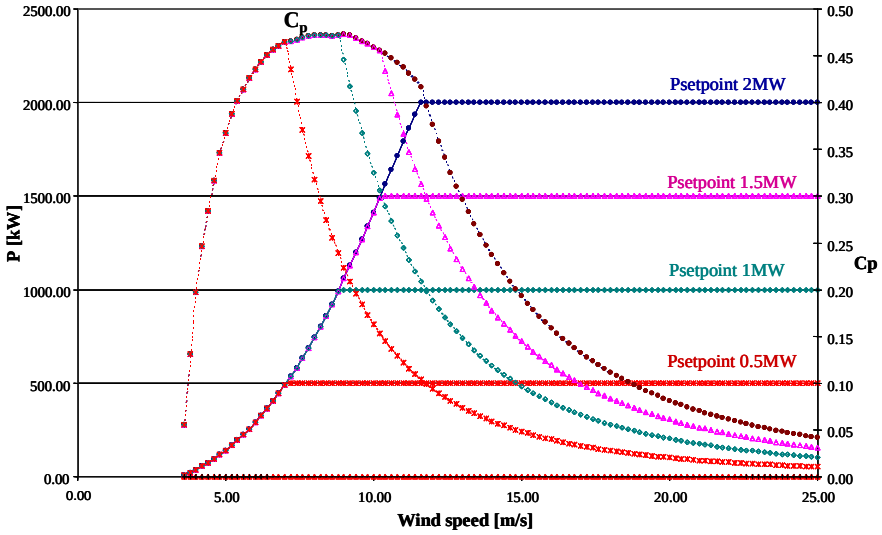

Figure 17: Power curves and C_p curves for different wind turbine power setpoints.

Notice that by imposing a power setpoint lower than the designed rated power of the wind turbine, the wind turbine range with high aerodynamic efficiency is, as expected,

reduced, while the maximum aerodynamic efficiency is moving toward lower wind speeds.

Early in the present project, a power control for an active stall wind turbine was developed and described by Jauch et.al. [21]. The early controller is general and designed to model a typical active stall turbine. However, the power control is relatively slow, mainly because it tries to reduce the pitch activity as much as possible to limit the stress of the pitch system. Such a controller design is not optimal for grid support, since in this case the wind farm is asked to act as a fast active element in the power system. To speed up the power control, a new active stall controller is presented and used here. The new power controller is actually simpler as will be seen below. To provide the best grid support, the aim is to use a power controller, which enables fast control of the wind farm power to different power setpoints imposed by system operator. Still, the pitch activities due to wind fluctuations are reduced, making the response to wind fluctuations slow.

Figure 18 illustrates the proposed power control scheme for an active stall wind turbine. A PI controller with anti wind-up ensures a correct active power production from the wind turbine both in power optimisation control mode and power limitation control mode. The input of the controller is the error signal between the measured active power at the Main Switch Point (MSP) (see Figure 16) and the active power reference p_{ref} imposed by the wind farm controller. The PI controller provides the pitch angle reference θ_{ref}, which is further compared to the actual pitch angle θ and then the error $\Delta\theta$ is corrected by the servomechanism. In order to get a realistic response in the pitch angle control system, the servomechanism model accounts for a servo time constant T_{servo} and the limitation of both the pitch angle and its gradient. The output of the actuator is the actual pitch angle of the blades.

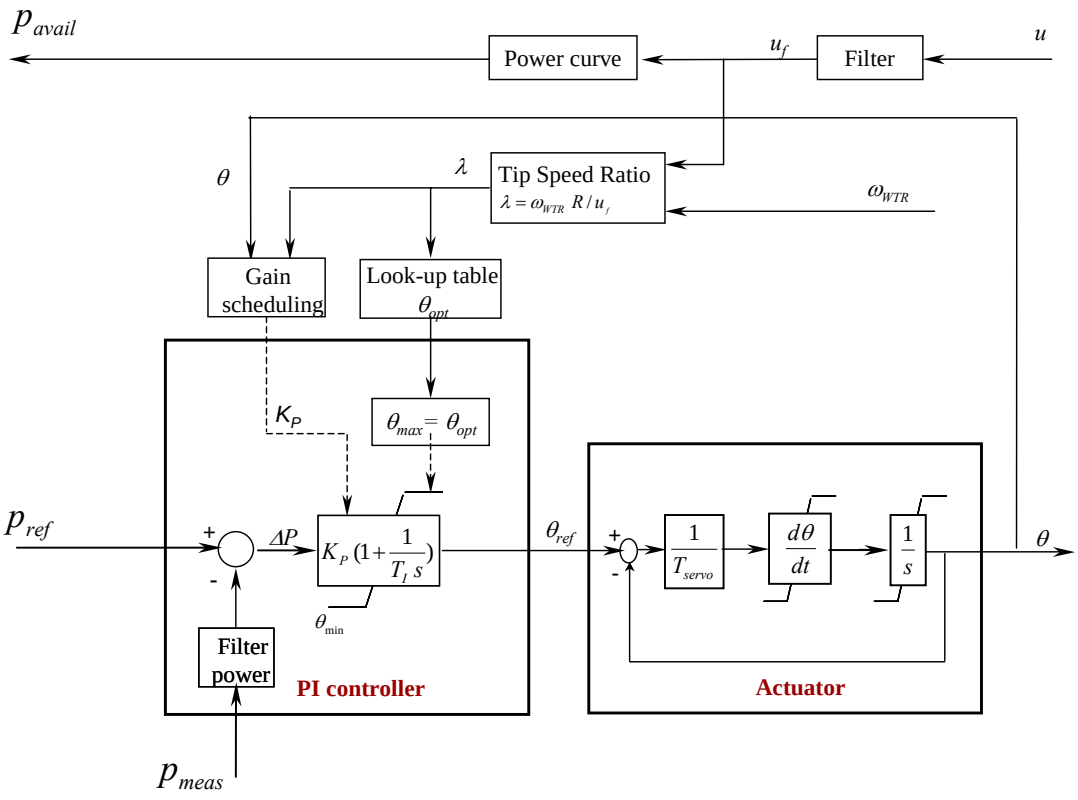

Figure 18: Proposed active power control scheme.

The information about the available power of the wind turbine, sent back to the wind farm controller at each instant, is expressed, as illustrated in Figure 18, based on the wind turbine's power curve and the filtered wind speed u_f. The wind speed is filtered appropriately to avoid unnecessary fluctuations.

In the power optimisation control mode, the controller has to maximise the power production. In this case, the difference between the measured power and its reference value is all the time positive and it is integrated up until the pitch reference angle reaches the upper limit of the controller. The optimal pitch angle is therefore used as the upper limitation of the controller. This upper limitation is calculated based on an "optimal pitch" look-up table as a function of the estimated tip speed ratio λ calculated according to (5) using the filtered wind speed u_f.

In the power limitation control mode, the error signal of the controller is negative and therefore the pitch angle is moving out the upper limitation and starts actively to drive the measured power to the power reference. Notice that the measured power used in the error signal is low-pass filtered in order to avoid that the 3p fluctuations in the power causes the pitch angle to fluctuate with the 3p frequency as well. This is because it is assumed that the pitch system is too slow to remove the 3p from the power, and thus the 3p fluctuations in the power would stress the system unnecessarily.

Compared to the controller presented in [21], the present controller contains furthermore an automatic gain scheduling control of the pitch angle in order to compensate for the existing non-linear aerodynamic characteristics. The gain scheduling is necessary to assure that the total gain of the system remains unchanged independent on the operational point of the wind turbine. The non-linear aerodynamic characteristics imply that the effect of pitching on the power varies depending on the operational point. The goal of the gain scheduling is therefore to change the proportional gain of the controller K_p in such a way that the total gain of the control loop remains unchanged independent on the operational point of the wind turbine. The pitch sensitivity, namely the effect of pitching, can be expressed mathematically by $\frac{dP}{d\theta}$. The total control loop gain K_{system} of the system can be then expressed as a proportional gain K_P in the PI controller times the pitch sensitivity of the system $\frac{dP}{d\theta}$, as follows:

$$K_{system} = K_P \frac{dP}{d\theta} = K_0 \left[\frac{dP}{d\theta}\right]^{-1} \frac{dP}{d\theta} = const. \qquad (9)$$

where K_0 is a dimensionless constant independent on the operation point.

The total gain of the system K_{system} is kept constant, by changing K_P in such a way that it counteracts the variation of the pitch sensitivity $\frac{dP}{d\theta}$ by the reciprocal sensitivity function $\left[\frac{dP}{d\theta}\right]^{-1}$, hence:

$$K_P = K_0 \left[\frac{dP}{d\theta}\right]^{-1} \quad (10)$$

The pitch sensitivity $\frac{dP}{d\theta}$ of the system depends on the operational point of the wind turbine. The operation point of the wind turbine is characterised directly by the wind speed and the power setpoint, and indirectly by the pitch angle and tip speed ratio. The implementation of the gain scheduling, namely the expression of the non-linear aerodynamic amplification in the system, is performed on-line based on the simulated pitch angle and tip speed ratio, according to:

$$\frac{dP}{d\theta} = \frac{1}{2} \rho \pi R^2 u^3 \frac{dC_p}{d\theta} \quad (11)$$

where u is the wind speed and the power coefficient $C_p = C_p(\theta, \lambda)$ depends on the pitch angle θ and the tip speed ratio λ. Figure 19 illustrates the pitch sensitivity for different wind speeds and power setpoints.

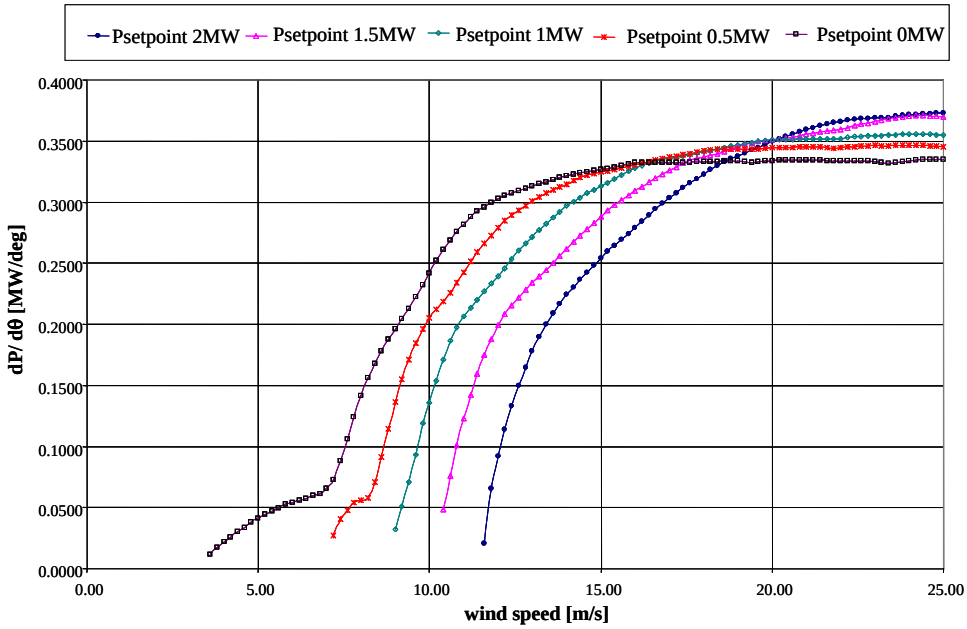

Figure 19: Pitch sensitivity function versus wind speed for different power setpoints.

Notice that the pitch sensitivity increases with increased wind speed. This shows that the more sensitive the system is (larger pitch angles θ / higher wind speeds) the smaller the gain for the controller should be and vice versa. When the active power setpoint is decreased, the pitch sensitivity increases at lower wind speeds.

Compared to [21], the present wind turbine controller contains in addition also a controller for the reactive power of the wind turbine. As illustrated in Figure 16, a capacitor bank is chosen to compensate for the reactive power absorbed by the induction generator or required by the grid operator. The reactive power consumption of an induction generator is a function of its loading and it increases as the active power

increases. The power factor of the induction generator at rated load is usually in the range of 0.85-0.90, which means that the consumption of reactive power is typically about half of the active power generation. This aspect is taken into account in the design of the size of the capacitor bank. In order to be able to produce reactive power to the grid the size of capacitor bank should be larger than the amount of reactive power consumed by the generator.

In the present implementation, a standard DIgSILENT SVC component is used to model the capacitor bank instead of a number of individual capacitors as used in earlier models by Sørensen et.al. [19]. The SVC component is a standard component in DIgSILENT, and it has the advantage of being an effective and easier way to simulate a capacitor bank consisting of several capacitor steps of the same size.

The standard SVC component is a combination of a shunt capacitor bank and a thyristor controlled reactance (TCR). The thyristor controlled reactance is usually used for a continuously control of reactive power. However, the compensation unit in wind turbines consists only of capacitors. Thus, the TCR part of the standard SVC component is deactivated in the present SVC control.

A discrete control of the capacitor bank is implemented using the dynamic simulation language DSL of DIgSILENT – see Figure 20. The capacitors in the capacitor bank can be switched on and off individually by the control system, depending on the load situation, in response to changes in the reactive power demand.

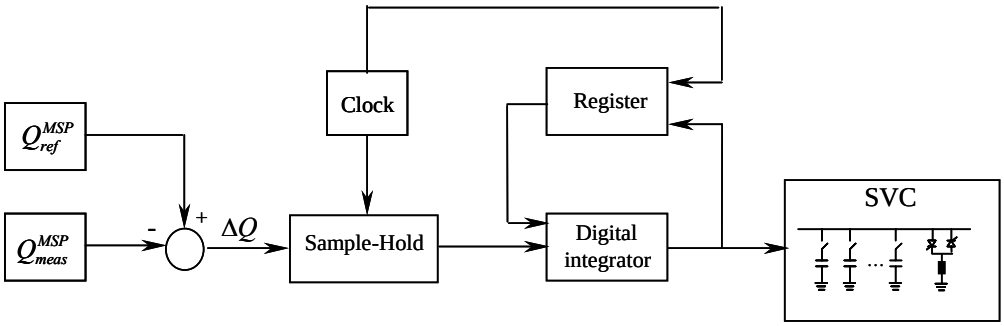

Figure 20: Designed capacitor bank control for the active stall wind turbine.

The difference ΔQ between the measured reactive power Q_{meas}^{MSP} on the low voltage side of the step-up transformer at the Main Switch Point MSP (see Figure 16) and the reference reactive power Q_{ref}^{MSP} imposed by the dispatch centre from the wind farm controller is used inside a sample-hold block. This block stores its sampled input signal at the output until the next rising edge of the clock signal appears. The clock supervises furthermore a register, which remembers the number of capacitors, which was switched on at the previous clock period. For each clock period, based on the new updated and the old loading situation, a digital integrator determines the needed number of capacitors.

The traditional wind turbines with directly connected induction generators are equipped with standard capacitor banks using mechanical contactors, which are typically controlled in intervals of 1-10 minutes. This control is not fast enough in the case when the turbine has to support the grid. If the capacitors were switched more often using mechanical contactors, the transients due to the switchings would reduce the lifetime of the capacitors and contactors too much. To provide a faster control possibility, new wind turbines use thyristor switches instead of mechanical contactors, which can reduce the

switching transients significantly and thus make it possible to switch the capacitor much more often without reducing the lifetime significantly.

As an example, the active stall controlled Bonus wind turbines in Nysted offshore wind farm in Denmark are equipped with such a dynamic phase compensation unit, using thyristor switches. Another similar dynamic phase compensation unit was tested on a wind turbine by Sørensen et.al. [22]. This test concluded that the dynamic phase compensation technology should not be used to remove the 3p fluctuations in reactive power, because the transients caused by the many capacitor switchings appeared to cause more flicker than could be removed by dynamically compensating the 3p reactive power fluctuations.

Thus, the control system of the capacitor bank has to switch the capacitors fast in order to be able to support the grid, but on the other hand it should not attempt to control the 3p fluctuations (three times the rotational frequency) in the reactive power consumption of the induction generator.

In the present work, the fast switching of the capacitors is assured by the clock time 20 ms, while the influence of the 3p fluctuations in reactive power is removed by implementing a hysteresis in the digital integrator. The hysteresis has been used instead of a low-pass filter in order to keep a very fast response to large changes in the reactive power reference. This is regarded important for the ability of the wind turbines to support the wind farm controller with voltage control.

Pitch controlled double fed wind turbines

A model of wind turbines and wind farms with doubly-fed induction generators has been developed and is presented e.g. in [23]. A doubly-fed induction generator is basically a standards wound-rotor induction machine with the stator windings directly connected to the three-phase grid and with the rotor windings connected to a back-to-back partial scale frequency converter, which consists of two independent converters connected to a common dc-bus. These converters are illustrated in Figure 21, as rotor side converter and grid side converter.

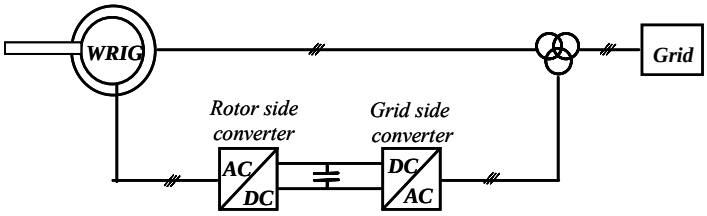

Figure 21: Doubly-fed induction generator system.

The behavior of the generator is governed by these converters and their controllers both in normal and fault conditions. The rotor side converter controls the rotor voltage in magnitude and phase angle, and is therefore used for active and reactive power control.

Figure 22 sketches the overall control system of a variable speed DFIG wind turbine implemented in DIgSILENT. Two control levels using different bandwidths can be distinguished:

- Doubly-fed induction generator (DFIG) control level
- Wind turbine control level

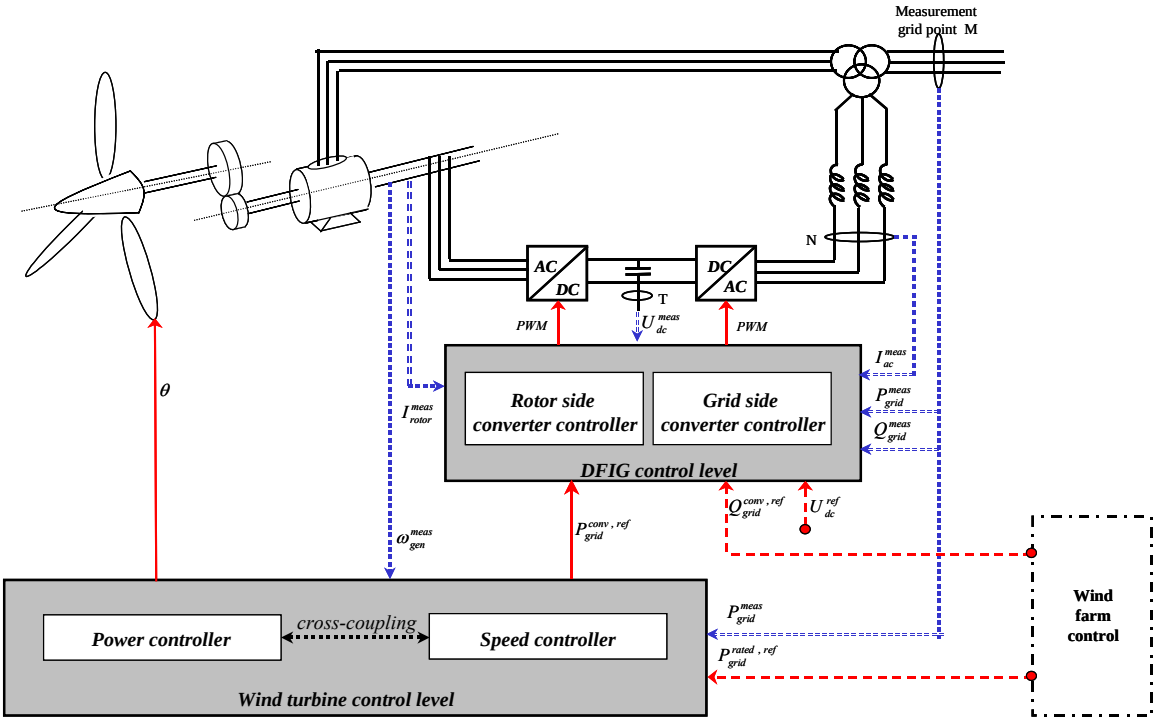

Figure 22: Overall control system of variable speed wind turbine with doubly-fed induction generator.

The DFIG control, with a fast dynamic response, contains the electrical control of the power converters and of the doubly-fed induction generator. The DFIG control contains two controllers:

- **Rotor side converter controller** - controls independently the active and reactive power on the grid point M – see Figure 22.
- **Grid side converter controller** - controls the DC link voltage U_{DC} and unity power factor to the grid through the rotor branch. The transmission of the reactive power from DFIG to the grid is thus only through the stator.

The wind turbine control, with slow dynamic response, provides reference signals both to the pitch system of the wind turbine and to the DFIG control level. It contains two controllers:

- **Speed controller** - has as task to control the generator speed at high wind speeds i.e. to change the pitch angle in order to prevent the generator speed becoming too. At low wind speeds, the pitch angle is kept constant to an optimal value.
- **Maximum power tracking controller** – generates the active power reference signal for the active power control loop, performed by the rotor side converter controller in DFIG control level. This reference signal is determined from the predefined characteristic P-ω look-up table, illustrated in Figure 23, based on filtered measured generator speed. This characteristic is based on aerodynamic data of the wind turbine's rotor and its points correspond to the maximum aerodynamic efficiency.

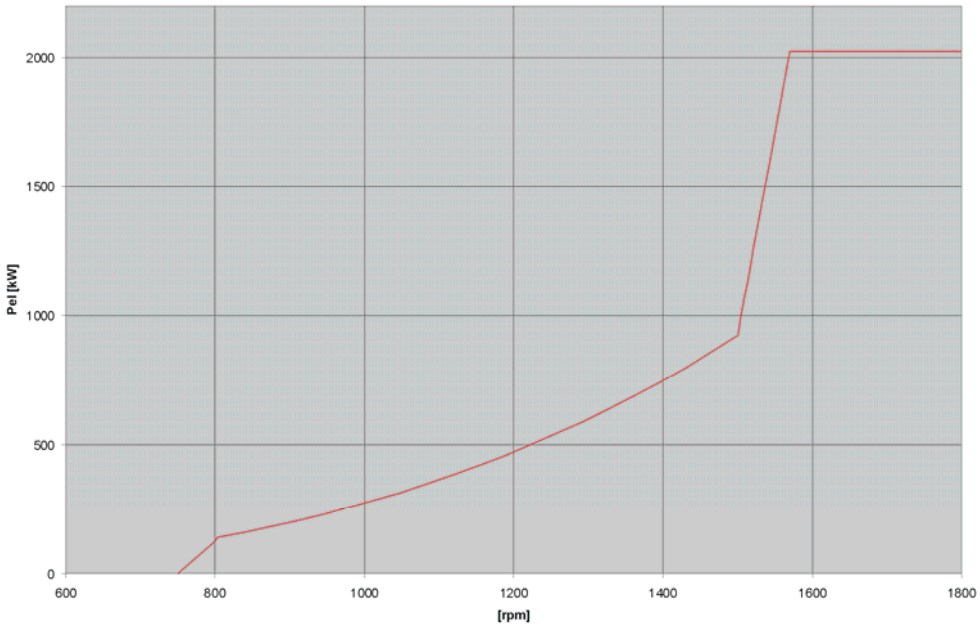

Figure 23: Power-omega characteristic used in the maximum power-tracking controller.

Both the speed controller and the maximum power-tracking controller are active in the power limitation strategy, while only maximum power tracking controller is active in the optimization power strategy. In the case of high wind speeds there is a cross coupling between these two controllers.

Figure 24 illustrates explicitly the speed controller, the maximum power tracking controller and the rotor side converter controller. The grid side converter controller does not interact directly with the wind turbine controller, and therefore it is shown as a "black box".

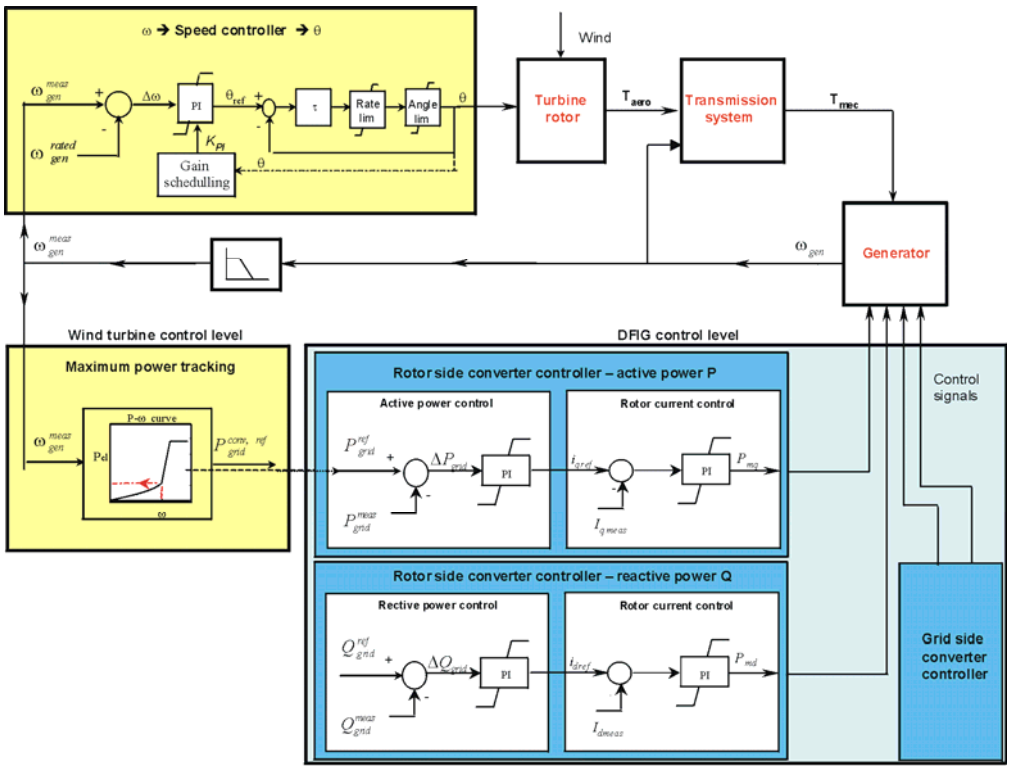

Figure 24: Wind turbine control level.

In the rotor side converter control, there are two independent control braches, one for the active power control and the other for reactive power control. Each branch consists of 2 controllers in cascade.

Notice that all these controllers, except maximum power tracking controller, are basically PI controllers. Both the speed controller and the maximum power tracking have as input the filtered measured generator speed. The generator speed is measured and a low-pass filter is used to avoid that the free-free frequency in the transmission system is amplified through the control system.

Speed controller implementation and design

The error between the filtered measured generator speed and the rated generator speed is thus sent to the PI speed controller. The output of this PI-controller is used as reference pitch signal θ_{ref} to the pitch system. In order to get a realistic response in the pitch angle control system, the servomechanism model accounts for a servo time constant T_{servo} and the limitation of both the pitch angle (0 to 30 deg) and its gradient (±10 deg/s). Thus the reference pitch angle θ_{ref} is compared to the actual pitch angle θ and then the error $\Delta\theta$ is corrected by the servomechanism.

A gain scheduling control of the pitch angle is implemented in order to compensate for the existing non-linear aerodynamic characteristics.

Active power control (rotor side converter controller)

The active power reference $P_{grid}^{conv,\,ref}$ signal, determined from the maximum power tracking look-up table, is further used in the active power control on the grid, performed by the rotor side converter controller.

The aim of the rotor side converter is to control independently the active and reactive power. The power is controlled indirectly by controlling the impressed rotor current. As illustrated in Figure 24, the active power control contains two control loops in cascade: a slower (outer) power control loop and a fast (inner) rotor current control loop. The slower power control loop has thus as output the reference rotor current signal, which is used further by the fast current control loop.

4.3 HVDC / VSC

The HVDC transmission system with Voltage Source Converter (VSC) has been developed as an alternative to the classical HVDC system due to some specific attributes such as: independent control of reactive and active power, continuous voltage and frequency regulation, black-start capability, etc [24], [25].

Currently two main concepts exist for such a transmission system. The first concept is the HVDC Plus developed by Siemens, which use two single 6-pulse converters to form a 12-pulse bipolar group as shown in Figure 25.

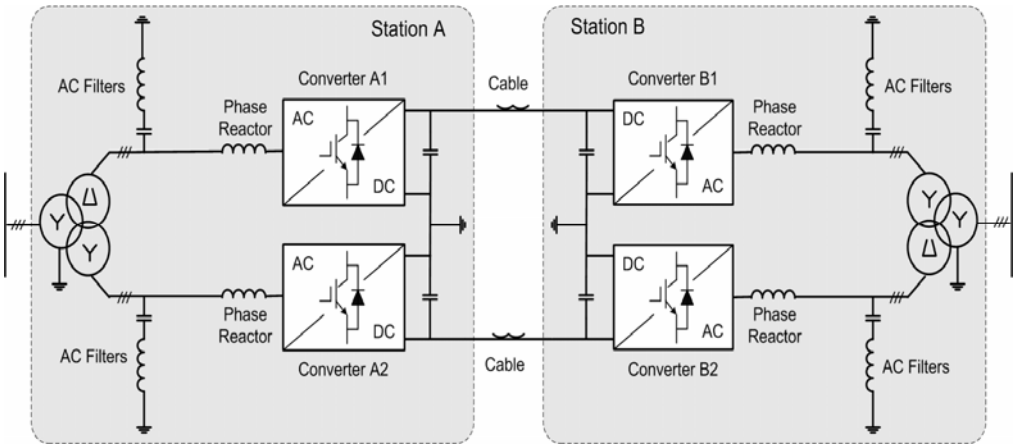

Figure 25. Main circuit diagram of a bipolar HVDC Plus transmission system.

This system is available for power ratings up to 200 MW for one bipolar unit with DC voltages up to ± 150 kV [24]. The second concept developed by ABB is the HVDC Light based on a 6-pulse bipolar VSC with ratings up to 330 MW/± 150 kV DC for one bipolar unit [25] as shown in Figure 26.

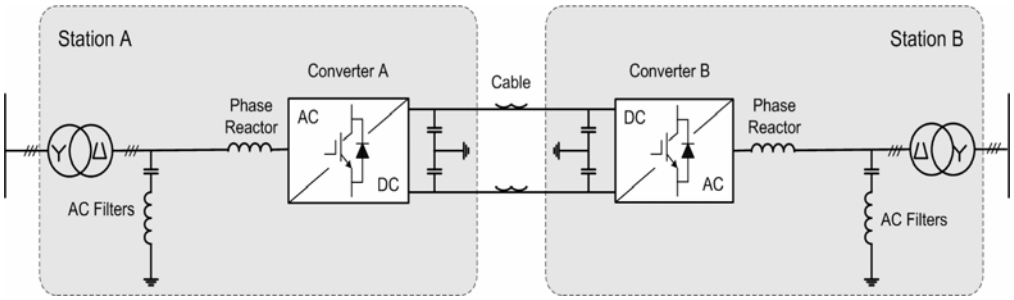

Figure 26. Circuit diagram for the HVDC Light transmission system

Both concepts have a four-quadrant operation in the P-Q plane and decoupled control for active and reactive power. This means that each converter can operate as rectifier or inverter at variable frequency and to absorb or deliver reactive power to the AC grid.

In 1998, Eltra decided to investigate the HVDC Light technology for DC connection of wind power to transmission grid. An HVDC Light transmission system was realized on the existing wind farm at Tjæreborg [26], [27].

The schematic of the Tjæreborg system including some basic data is shown in Figure 27.

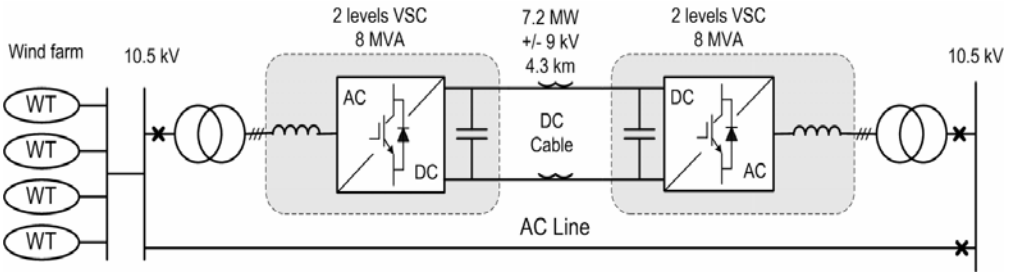

Figure 27. Schematic of the Tjæreborg transmission system.

The Tjæreborg wind farm consists of 4 different type of wind turbine with different nominal powers. Two of these turbines are pitch regulated (type B and type C) while the other two are stall controlled (type A). The rated power of the wind farm is 6.5 MW [27] while the HVDC system is 8 MVA rated.

The DC transmission system is in parallel with an AC line and it has a length of 4.3 km. The voltage and frequency in the wind farm can be varied continuously and independently of the transmission grid [26], [27] using this DC link. In isolated operation the frequency can vary between 30 and 65 Hz [26].

According with [26] the control concept was implemented and tested in EMTDC program under different conditions and it has been found a “fairly good agreement between simulation and commissioning tests”. However, the frequency control of the wind farm was an exception. In simulation the dynamic frequency control worked fine [26]. During the commissioning test the frequency was varied between 47 and 51 Hz. Outside this range the wind turbines are tripped by their protections [26]. In [26] is mentioned that a reason for different result in simulation compared with the commissioning tests might be the difficulties in simulating correctly the dynamics of the wind farm. Also the following remark should be noticed “with a stiff voltage concept the interaction between the HVDC Light and the windmills is much more robust and simple”.

Built-in model of PWM converter in DIgSILENT

The PWM converter model represents a self-commutated, voltage source AC/DC converter based on the equivalent circuit shown in Figure 28 [28]. The DC-link capacitor is not included in the converter model.

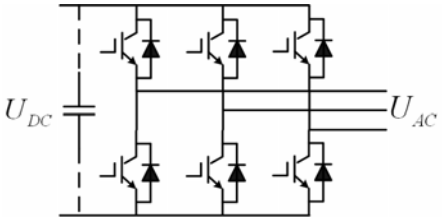

Figure 28. Equivalent circuit of the PWM converter.

The model supports sinusoidal and rectangular modulation. Saturation and losses are taking into account. An equivalent resistance between the DC terminals models the losses in the converter.

This model is based on a fundamental frequency approach for all steady-state functions including RMS and EMT simulations.

In all steady-state functions, including RMS-simulation, real and imaginary parts of the AC-voltage correspond to the positive sequence component. In EMT-simulation, it corresponds to the space-phasor [28].

Load flow analysis

This model in load flow analysis supports several control conditions. The initial value of the PWM modulation index results from the load flow calculation. The supported control conditions are as follows:

- V_{ac}-phi – Specifies magnitude and phase of the AC terminal. Typical control mode for motor-side converters in variable speed applications.
- V_{dc}-phi – Specifies the DC-voltage and the AC-voltage phase. No typical application;
- PWM-phi – Load flow setup without control. The PWM index is directly set in magnitude and phase.
- V_{dc}-Q – Specifies DC-voltage and reactive power. Typical applications: STATCOM, UPFC, grid-side converter for doubly-fed induction machine, VSC-HVDC applications.
- V_{ac}-P - Specifies AC-voltage magnitude and active power. This mode is equivalent to a PV characteristic of synchronous generators. Typical applications: Grid-side converter of converter driven synchronous machines, VSC-HVDC;
- P-Q – Specifies P and Q at the AC-side. This control is equivalent to a PQ characteristic of synchronous machines. Typical applications: Grid-side converter of converter driven synchronous machines, VSC-HVDC.

Since the model is based on the fundamental frequency approach, the load flow calculations will assume always a 50 Hz frequency on the bus bars. Then, the voltage angle for each bus bar is calculated in respect with the global reference frame as shown in Figure 29. This is the reason that for all the control conditions in the load flow analysis the frequency is not a controlled variable.

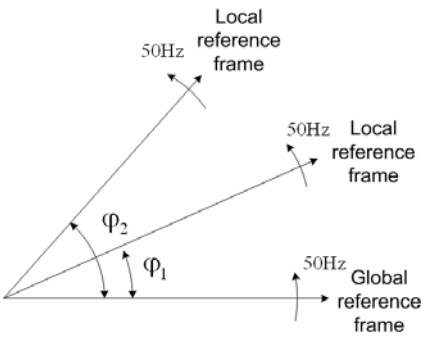

Figure 29. Reference systems in DIgSILENT.

Stability model (RMS)

The stability model is equivalent to the fundamental frequency model. The PWM index (magnitude and phase) can be defined in different ways depending on the application. First the input definition for this stability model will be presented. This will help to understand better the possible control methods and typical applications of the PWM converter in DIgSILENT.

The input definitions of the stability model (RMS) are presented in Table 4.

Name	Unit	Description
Pm_in	p.u.	Magnitude of PWM Index
f0	p.u.	Input frequency
F0Hz	Hz	Input frequency
dphiu	rad	Voltage angle
Pmr		Real part of PWM index
Pmi		Imaginary part of PWM Index
cosref		Cos of reference angle
sinref		Sin of reference angle
Pmd		PWM Index in d-axis
Pmq		PWM Index in q-axis
id_ref	p.u.	Current reference in d-axis
iq_ref	p.u.	Current reference in q-axis

Table 4. Input definition of the stability model

The control variables for the stability model are defined in 4 ways depending on the applications [28]:

A. *Pmr*, *Pmi* – Real and imaginary part of the PWM index. The reference system in this case is the global reference frame, which is usually defined by a reference machine, external network, voltage source or a PWM converter. This sets of

inputs must be always used in combination with phase measurement devices e.g. Phase Locked Loop (PLL) and transformation between reference frames.

B. *Pmd, Pmq*, *cosref*, *sinref* – This set of input is used in grid-connected applications. The PWM Index-vector is specified with a reference to a reference system, which is defined by *cosref* and *sinref*. For example the output from the current controllers are connected to *Pmd* and *Pmq* while the voltage is measured using a PLL and its output gives the *cosref* and *sinref* signals.

C. *Pm_in*, dphiu – magnitude and phase of the PWM Index. This representation is equivalent to Pmr, Pmi. The phase of PWM Index *dphiu* is expressed with reference to the global reference frame.

D. *Pm_in*, *f0* (*F0Hz*) – *Pm_in* is the magnitude of the PWM index and *f0* permits varying the frequency of the output voltage. The control variable *f0* defines the frequency in p.u., while *F0Hz* in Hz. According with [28] this input pair "is especially useful in variable speed-drive applications, in which a PWM converter is used for driving an induction machine".

Based on these available control variables for the PWM-converter model, the following can be concluded:

- Options A to C can only be used in grid-connected applications. In order to obtain the right angle for the output voltage these options requires a phase measurement device (e.g. PLL). Transformations between reference frames should be made for option A and B. ***The frequency of the output voltage cannot be varied using these options!*** This will be in all the cases around 50 Hz. The control schemes associated with these options will control only the magnitude and the phase of the output voltage.
- Option D is the only possibility to vary the frequency of the output voltage in a wide range. Using this option, it is not possible to use vector control schemes. The only control scheme associated with this input pair should be similar with the scalar control (V/f control) for drives.

The control schemes for the DC transmission system developed in DIgSILENT during this project take into account all the above-mentioned aspects. In the following paragraphs these schemes are presented in detail.

Control for Station A (sending end station)

The main target here was to implement a control scheme, which must provide voltage and frequency set points for the wind farm controller. Therefore, the magnitude of the PWM index and the frequency (Pm_in, f0) are used as control variables for the PMW converter model. Since each wind turbine can have different values for the wind speed in a given moment and therefore different operation points a droop control for both voltage and frequency has been adopted as shown in Figure 30.

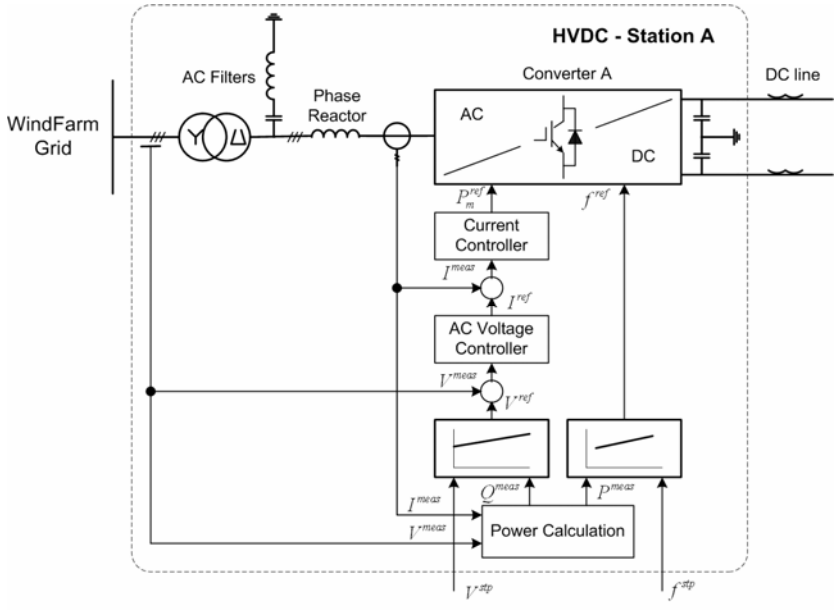

Figure 30. Structure of the control for sending end station (wind farm side).

Each wind turbine will deliver active power and will absorb reactive power according with the wind speed variations. Therefore the voltage stability is dependent on the demand for reactive power [29]. The voltage control loop should ensure that the reactive currents, which circulate inside the wind farm, are not large. A droop characteristic for the voltage controller will minimize the stationary error in this case. Since the induction generator will always draw reactive power from the PWM converter, the reference for voltage should be increased when the generator demand for reactive power increase as shown in Figure 31.

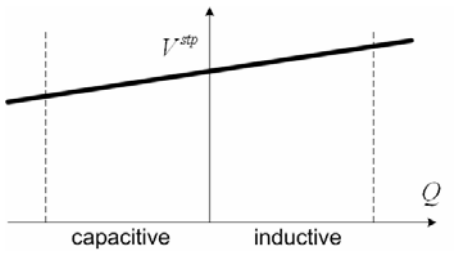

Figure 31. Voltage set point with droop characteristic.

The voltage reference value is calculated using:

$$V^{ref} = V^{stp} + k_v Q^{meas} \tag{12}$$

where k_v is the voltage droop coefficient.

An inner current control loop will assure a relatively fast tracking of the actual current.

A collective variable speed operation of the connected wind turbines is introduced using a frequency droop characteristic. The set point frequency is varied as a function of the produced power as shown in Figure 32.

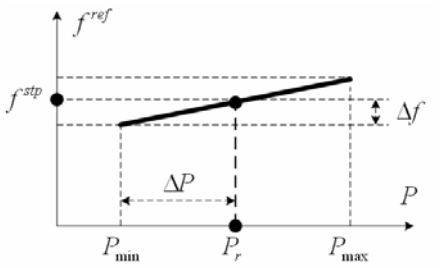

Figure 32. Frequency set point with droop characteristic.

The reference for frequency is given in per unit as:

$$f^{ref} = 1 - k_f(1 - P^{meas}) \tag{13}$$

where k_f is the droop coefficient for frequency defined as

$$k_f = \frac{\Delta f}{\Delta P} \tag{14}$$

Control for Station B (receiving end station)

Usually in grid-connected applications the PWM converter from the grid side must control the DC-link voltage and the reactive power. Therefore for the receiving end station of the considered DC transmission system such a control scheme is implemented in DIgSILENT.

Several DC-link voltage control schemes exist depending on the application [30]. There are two topologies commonly used namely master/slave and droop control. The master/slave control is used for parallel operation of converters. The active load sharing is performed and the master controller distributes references for power to other converters (slave). Since this control requires communications between converters the bandwidth of the DC link voltage control can be increased if the communication bandwidth is relatively high [30]. In this way less energy needs to be stored in the DC bus and therefore the DC capacitance can be decreased. In [30] is mentioned that the system become sensitive to interactions between the two sides when the energy storage is reduced.

In the droop control each converter delivers power to the DC bus determined by the actual DC bus voltage error at the converter [30]. This control method does not require communication between converters.

Since the PWM converter can be seen as a controlled voltage source the equivalent diagram of the receiving end station is as shown in Figure 33.

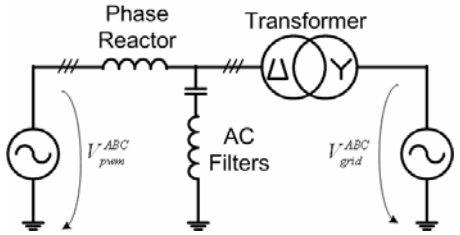

Figure 33. Equivalent diagram of the receiving end station.

As the station operates around 50 Hz grid frequency all the time the influence of the capacitors can be neglected. Therefore, the equivalent diagram of the station can be reduced as shown in Figure 34.

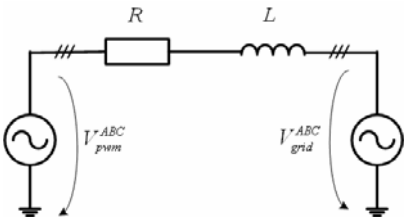

Figure 34. Simplified diagram of the receiving end station neglecting the AC filters.

The voltage equations can be written as:

$$v_{grid}^{ABC} = R \cdot i^{ABC} + L\frac{di^{ABC}}{dt} + v_{pwm}^{ABC} \tag{15}$$

Assuming that the voltage system is symmetrical and balanced the zero component can be neglected in stationary reference frame. Therefore (15) can be written as:

$$v_{grid}^{\alpha\beta} = R \cdot i^{\alpha\beta} + L\frac{di^{\alpha\beta}}{dt} + v_{pwm}^{\alpha\beta} \tag{16}$$

Further in the synchronous reference frame it is assumed that $\frac{d\omega_{grid}}{dt} = 0$, and (16) can be written in matrix form as:

$$\begin{bmatrix} v_{grid}^{d} \\ v_{grid}^{q} \end{bmatrix} = L\frac{d}{dt}\begin{bmatrix} i^{d} \\ i^{q} \end{bmatrix} + \begin{bmatrix} 0 & -\omega_{grid} \cdot L \\ \omega_{grid} \cdot L & 0 \end{bmatrix} \cdot \begin{bmatrix} i^{d} \\ i^{q} \end{bmatrix} + \begin{bmatrix} v_{pwm}^{d} \\ v_{pwm}^{q} \end{bmatrix} \tag{17}$$

It can be observed that there is a cross coupling between axes with the term $\omega_{grid}L$. A change of the current e.g. in d-axis results in a change of the q-axis current. Therefore, this cross coupling should be taken compensated in the control scheme.

In this project a droop control of the DC-link voltage is implemented for the receiving end station as shown in Figure 35. The entire control scheme is build in dq-system. Therefore a PLL is used to calculate the angle for transformations between axes. The actual power from the DC-link is calculated based on the measured voltage and power. Another measurement block in the connection point delivers the signals for reactive power calculation.

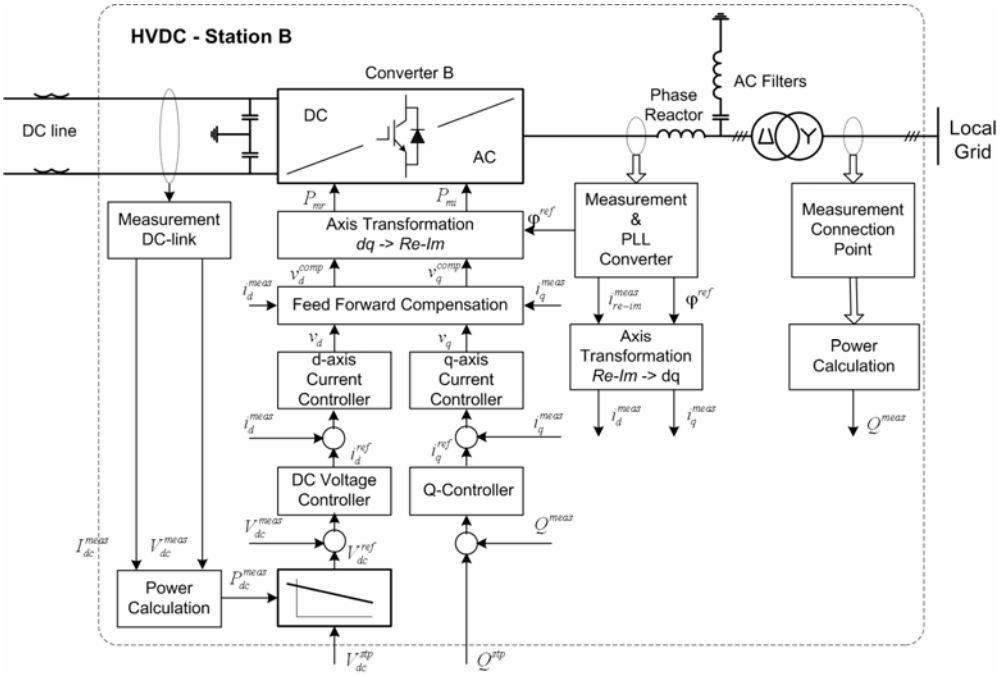

Figure 35. Control structure of the receiving end station (grid side).

The DC-link voltage set point is calculated using the actual active power from the DC-link and the droop characteristic. A 5% variation in DC-link voltage is allowed. The error signal between set point and the measured value fed the PI controller. One of the advantages of using the PI controller is the error restoration in droop control [30]. The output from DC-link voltage controller is the reference for current in d-axis. The error between the reactive power set point and the actual value is applied to a PI controller, which gives the reference for the q-axis current.

The control scheme comprises also an inner current control loop for both axis and a feed-forward compensation of the voltage references (modulation index in d and q axis). The feed-forward compensation requires the exact value of the total reactance connected between PWM converter and the connection point in the grid. This reactance is the sum of the phase reactor and transformer reactances.

The transformer reactance has been calculated based on:

$$Z_T = \frac{\Delta u_k \cdot U_n^2}{100 \cdot S_n} \tag{18}$$

$$R_T = \frac{\Delta P_{Cu} \cdot U_n^2}{1000 \cdot S_n} \tag{19}$$

where:

- Δu_k - short circuit voltage [%];
- U_n - rated voltage [kV];
- S_n - rated apparent power [MVA];

- ΔP_{Cu} - copper losses [kW].

Without the feed-forward compensation the reactive power cannot be controlled accurately.

The reactive power set point is given so that the reactive power flow in the connection point is kept at zero. However, other values for this set point can be imposed by the wind farm controller.

5 Wind farm control strategies

5.1 Active/combi stall controlled wind turbines with AC transmission

This section describes a wind farm controller, which can in principle work on any wind turbine, although it has only been simulated using wind turbines with active stall wind turbines as described in section 4.2.

Figure 36 illustrates the diagram of the wind farm control level. The wind farm control level behaves as a single centralized unit. It has as input signals demands from the system operator, measurements from the point of common coupling (PCC) and available powers from the wind turbines. The available power of each wind turbine is determined at the wind turbine level based on the wind turbine's power curve and an estimated wind speed. The system operator can order the wind farm to operate either with normal (maximum) production or with limited production.

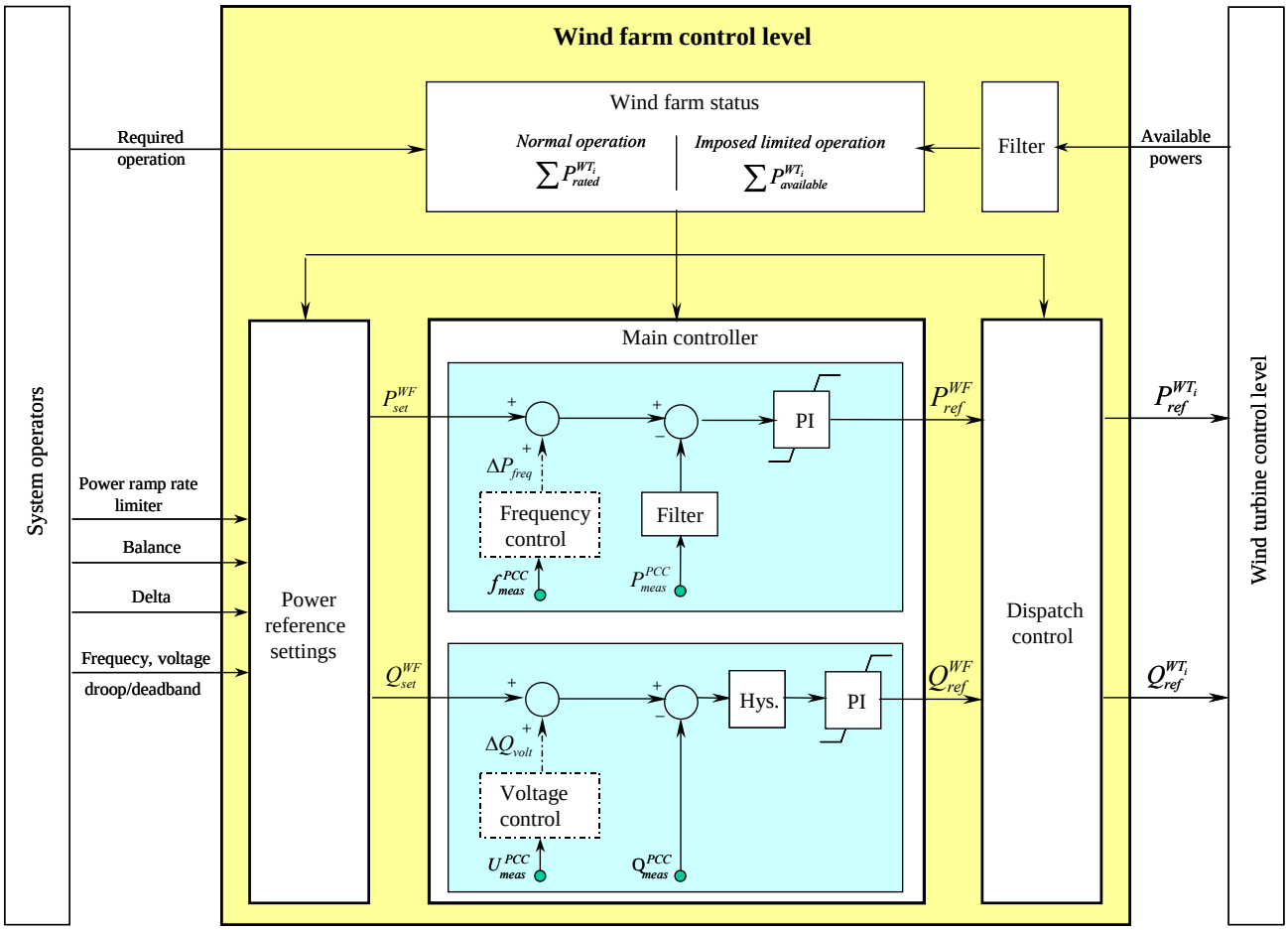

Figure 36: Wind farm control for the active stall wind farm.

The system operator also decides how fast the wind farm production should be adjusted (power ramp rate limiter), and if there is a need for a reserve capacity (balance and/or delta control), a frequency and a voltage control. The power ramp rate limiter reduces both the positive and negative excessive power ramp rates in the active power of the wind farm. Based on all these requirements from the system operators, the wind farm controller elaborates the power reference signals for each individual wind turbine control.

The wind farm control system contains typically a power reference settings block, a wind farm controller itself and a dispatch function block. At the present stage, delays due to the signal communication between the wind farm control level and the wind turbines are neglected.

In the power reference settings block, different control functions for active and reactive power, as illustrated in Figure 36, are implemented in such a way that they can be active at the same time. There are two concomitant control loops in the wind farm controller itself: one for the active power control and the other for the reactive power control. The active control loop is based on a controller for the active power and a subordinated frequency control loop, while the reactive control loop is based on a controller for the reactive power and a subordinated voltage control.

The principle of the active and reactive power control loops is as follows. First an active and reactive power reference signal (P_{set}^{WF} and Q_{set}^{WF}), respectively, are elaborated in the

power reference settings block, based on one or several control functions required by the system operator. These reference signals can be, if necessary, adjusted further with some corrections ΔP_{freq} and ΔQ_{volt} from the subordinated control loops (frequency and voltage), in order to support power system control of frequency and voltage in PCC.

In the case when only the wind farm's capability to control the wind farm's active and reactive power production, i.e. secondary control capability is in focus, the frequency and voltage subordinated control loops can be neglected, their corrections being assumed zero.

Each control loop consists of a PI controller with anti wind-up that ensures a correct power production from the wind farm. The controller computes a power error and sets up the power reference (P_{ref}^{WF} , Q_{ref}^{WF} respectively) for the whole wind farm.

Notice that only the active and not the reactive power signal is low-pass filtered in order to avoid that the 3p fluctuation is amplified through the control system. Fast variations in the reactive power reference from the wind farm controller, due to 3p fluctuations, are removed using a hysteresis in the wind farm control level – see Figure 36. This is because the speed of the reactive power control has priority above the accuracy, in order to take full advantage of the fast response of the dynamic phase compensation. For active power control, the blade pitching will anyway slow down the possible control speed, and therefore a 3p filter will not slow down the active power control significantly more.

A dispatch function block converts further the power reference signals from the controller into power reference signals for each individual wind turbine of the wind farm. There are different ways to design the dispatch function but the one presented in this paper simply distributes the power references to the wind turbines $P_{ref}^{WT_i}$, $Q_{ref}^{WT_i}$ (*i=1:n*) based on a proportional distribution of the available active power and maximum reactive power, respectively:

$$P_{ref}^{WTi} = \frac{P_{av}^{WTi}}{P_{av}^{WF}} P_{ref}^{WFC}, \qquad Q_{ref}^{WTi} = \frac{Q_{\max}^{WTi}}{Q_{\max}^{WF}} Q_{ref}^{WFC} \tag{20}$$

where the total active power and the maximum reactive power of the wind farm are expressed as follows:

$$P_{av}^{WF} = \sum_{i=1}^{n} P_{av}^{WT_i}, \qquad Q_{\max}^{WF} = \sum_{i=1}^{n} Q_{\max}^{WT_i} \tag{21}$$

and where $P_{av}^{WT_i}$ is the available power for the *i'th* wind turbine in one specific point in time. $Q_{\max}^{WT_i}$ is the maximum possible reactive power for the *i'th* wind turbine.

Notice in Figure 36 that all three mentioned blocks in the wind farm controller (power reference settings block, main controller block and dispatch block) have an upper limited supervisory signal, depending on the wind farm status. In normal operation, i.e. when the wind farm should produce maximum power, the upper limited signal is constantly equal to the rated power of the whole farm, while in limited operation this signal is given by the sum of the available power of each individual wind turbine. The available power received from each wind turbine is low-pass filtered in order to avoid that the 3p frequency is amplified through the control system. The reason why the upper limited signal is equal to the total rated power of the whole wind farm in normal operation is,

that if the limit was equal to the available power, the wind turbine would pitch unnecessarily to limit the power to the estimated available power.

5.2 Pitch controlled double fed wind turbines with AC transmission

This section describes a wind farm controller, which can in principle work on any variable speed wind turbine, although it has only been simulated using wind turbines with doubly-fed induction generator. This controller was actually developed before the controller presented in section 5.1, and it will not work properly with fixed speed wind turbines. The reason is that it uses wind turbine available power as wind turbine reference power when maximum power is requested. The general wind farm controller in section 5.1 uses the rated power instead of available power as reference to request maximum power as explained above.

The wind farm controller has to take over the determination of the wind turbine power set point to be able to perform power control. But when the wind farm controller is not intended to limit the wind turbine power production, it is important that maximum power is still obtained. The present wind farm controller is designed to maintain the robust maximum power point tracking of the power-speed control scheme, as long as the power is not limited by the wind farm power control.

A block diagram of the wind farm controller is shown in Figure 37 together with the modified wind turbine power controller. Essentially, the power control loop in the wind turbine controller in Figure 24 is opened at the "wind turbine control level", which makes it possible for the wind farm controller to set the power reference in the wind turbine. Besides, the output of the "maximum power tracking" power – speed table, which is not used as wind turbine power reference any more, is now send to the wind farm controller as available instantaneous power, P_{avail}^{inst} (Figure 37).

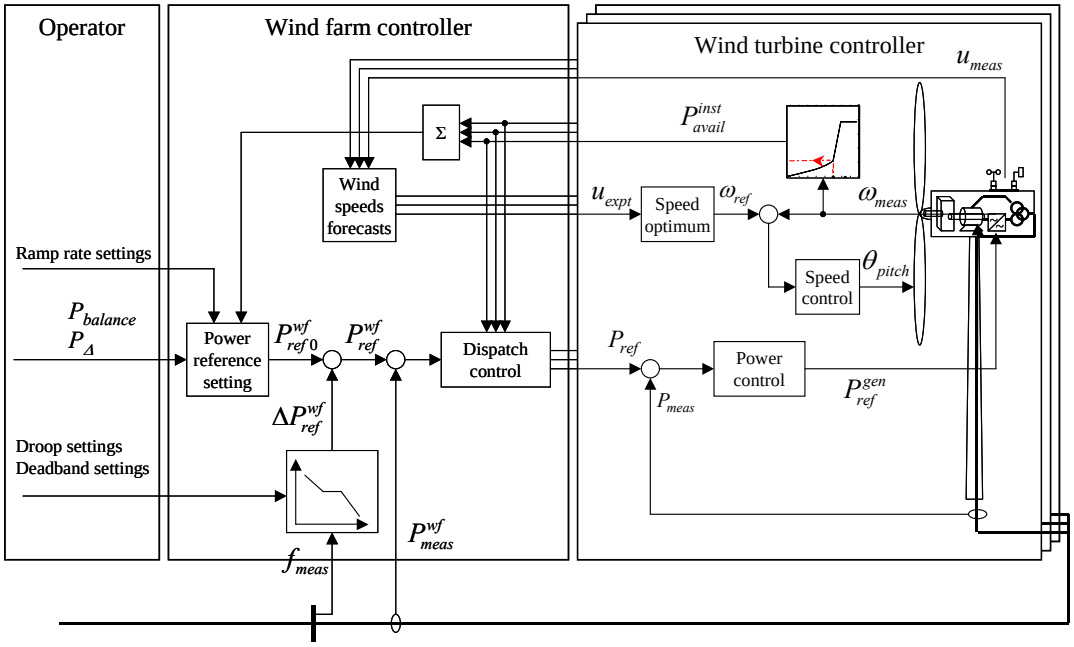

Figure 37 Model for wind farm power contoller with DFIG technology.

If the power is not limited by active balance, delta or ramp control, the wind farm controller will return the available power as set point to the wind turbine, P_{ref}. This is done in the way that the wind farm controller sums the available power from all wind

turbines and uses that sum as reference for the wind farm power, P_{ref}^{wf} . The "dispatch control" block in Figure 37 simply distributes the power references to the wind turbines, proportionally to the distribution of available power.

This concept is very robust to maximum power point tracking, because it works like the autonomous wind turbine controller in Figure 24, but only with a small delay due to transmission of signals between wind turbine and wind farm controller.

If the power is limited, by ramp rate, balance or delta control, P_{ref}^{wf} is reduced to less than the sum of available power. As a consequence, the dispatch control will reduce the individual reference signals P_{ref} to the wind turbines.

Now, if the reference to the speed controller wind the wind farm control in Figure 37 was ω_{gen}^{rated} as with autonomous wind turbine control in Figure 24, the wind turbine would use the surplus power to accelerate to ω_{gen}^{rated} before the speed controller would pitch to limit the speed. This would cause higher fatigue loads on the wind turbine when the power control is taken over by the wind farm controller, because the rotational speed would be higher. To avoid this, a "speed optimum" block sets the reference speed continuously depending on the wind speed. An advanced wind speed forecast can be applied to provide the wind speed input to the speed optimum block, but because of the results in section 2.4 of this report, the wind speed input is simply obtained by filtering the measured wind speed from the wind turbine.

The frequency control and voltage control have also been implemented in the simulation model. The frequency control is shown in Figure 37. The voltage control is also done by the wind farm controller, which will determine the setpoints for the reactive power in the wind turbines. The reactive power control on the wind farm level is quite similar to the active power control, using available reactive power from each wind turbine in a dispatch block, which distributes the required reactive power between the wind turbines to obtain the required reactive power or voltage in the PCC.

5.3 HVDC/VSC transmission and active/combi stall controlled wind turbines

HVDC with voltage source converters, described in section 4.3, provide the ability to control the reactive power independently on the grid side (receiving) converter. The reactive power consumption of the wind turbine induction generators can in this case be provided by standard, thyristor switched capacitor banks, because the wind farm side (sending) converter will provide the necessary balancing of reactive power to the wind farm grid.

The wind farm controller presented in section 5.1 can be applied to this concept. Only, the reactive power control of the individual wind turbines should be performed by the wind turbines, independently on the wind farm controller. Instead, the wind farm controller should set the reactive power reference to the grid side converter of the HVDC.

The wind farm controller with grid support according to the functional description in chapter 3 has not been implemented and tested with the HVDC concept in the present work. The HVDC wind farm model has been built on an early stage in the project, with autonomous active and reactive power control of the active stall wind turbines, using the original model with slow power control response [21].

Instead, a wind farm controller for variable speed operation with maximum power tracking was been implemented [31], [32], [33].

6 Simulation examples

6.1 Active/combi stall controlled wind turbines with AC transmission

Different scenarios are simulated to illustrate the performance of both the developed active stall wind turbine controller and the wind farm controller. Two sets of simulations are thus presented. The first set has as focus the power control of the individual active stall wind turbine, while the second set of simulations reveals how the wind farm controller controls the wind farm power production to the reference power ordered by the system operators. The controller's performance is assessed and discussed by means of normal operation simulations of the considered 6 MW wind farm connected to a strong grid. The simulation results are illustrated at the wind farm level and/or at the wind turbine level, depending on their information content.

Figure 38, Figure 39 and Figure 40 present simulation results of the proposed power control strategy of the active stall wind turbine, shown in Figure 18 and Figure 20, respectively. The active stall wind turbine is simulated at an average wind speed of 11 m/s and a turbulence intensity of 20%. This operational point for the wind turbine corresponds to a transition operational regime for the wind turbine, between power optimization and power limitation regime, where the 3p fluctuation (three times the rotational frequency) is strong.

The first plot in Figure 38 shows the reference power P_{ref}, the measured power P_{meas} in MSP and the filtered measured power P_{filt} used in the controller, while the other two plots illustrate the pitch angle and generator speed, respectively. As expected for an active stall wind turbine, the 3p fluctuation is present in the measured electrical power P_{meas}. In order to illustrate the performance of the active stall wind turbine controller, the following sequence is assumed. The first 60 sec, the power reference is set to the rated power (i.e. 2 MW). The power reference is then stepped down to 0 MW and after 120 sec it is stepped back again to 2 MW.

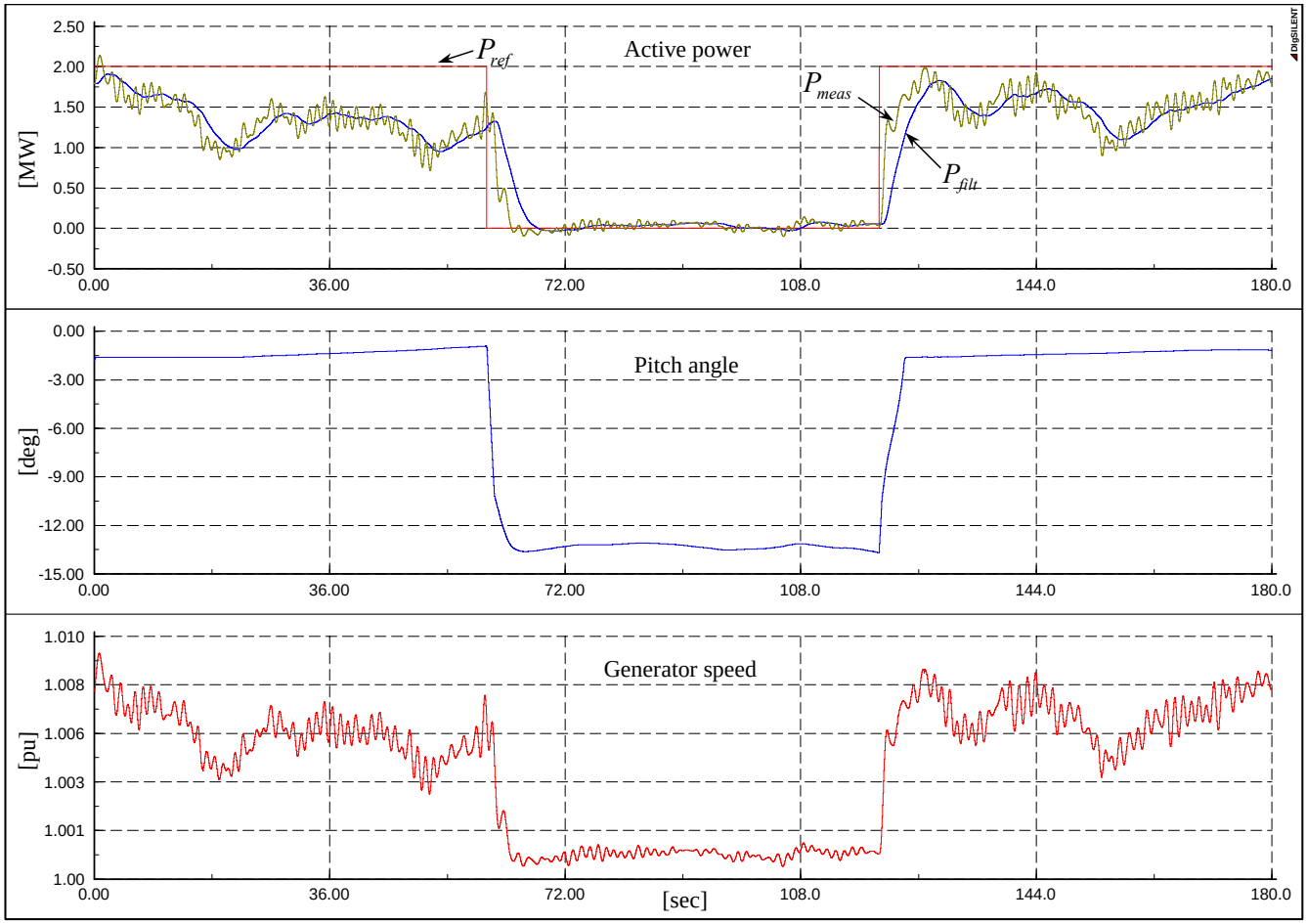

Figure 38: Power reference response of an active stall controlled wind turbine.

In the first and last 60 sec of the simulation, by setting the power reference equal to the rated power for a wind speed less than the rated wind, the wind turbine has to produce maximum possible power. In this case the pitch angle is set by the upper limit of the controller given by the "optimal pitch" look-up table – see Figure 18. The wind turbine is then ordered to work in the power limitation mode, when the power reference is set to 0 MW. In this control mode, the turbine has to produce less than it is capable of and therefore the power controller starts actively to change the power to the power reference, which can be seen on the measured power. The controller has been tuned so that the pitch angle changes smoothly from one steady state operational point to another without any overshoot. A reduction of the power production implies a more negative pitch angle and a smaller generator speed (slip).

Figure 39 gives a more detailed view on the power and the pitch angle in the moment when the power reference is stepped down to 0 MW. The new power reference is reached in approximately 4 seconds. The change in the pitch angle is limited to ±8 deg/sec by the pitch rate limiter modelled in the actuator.

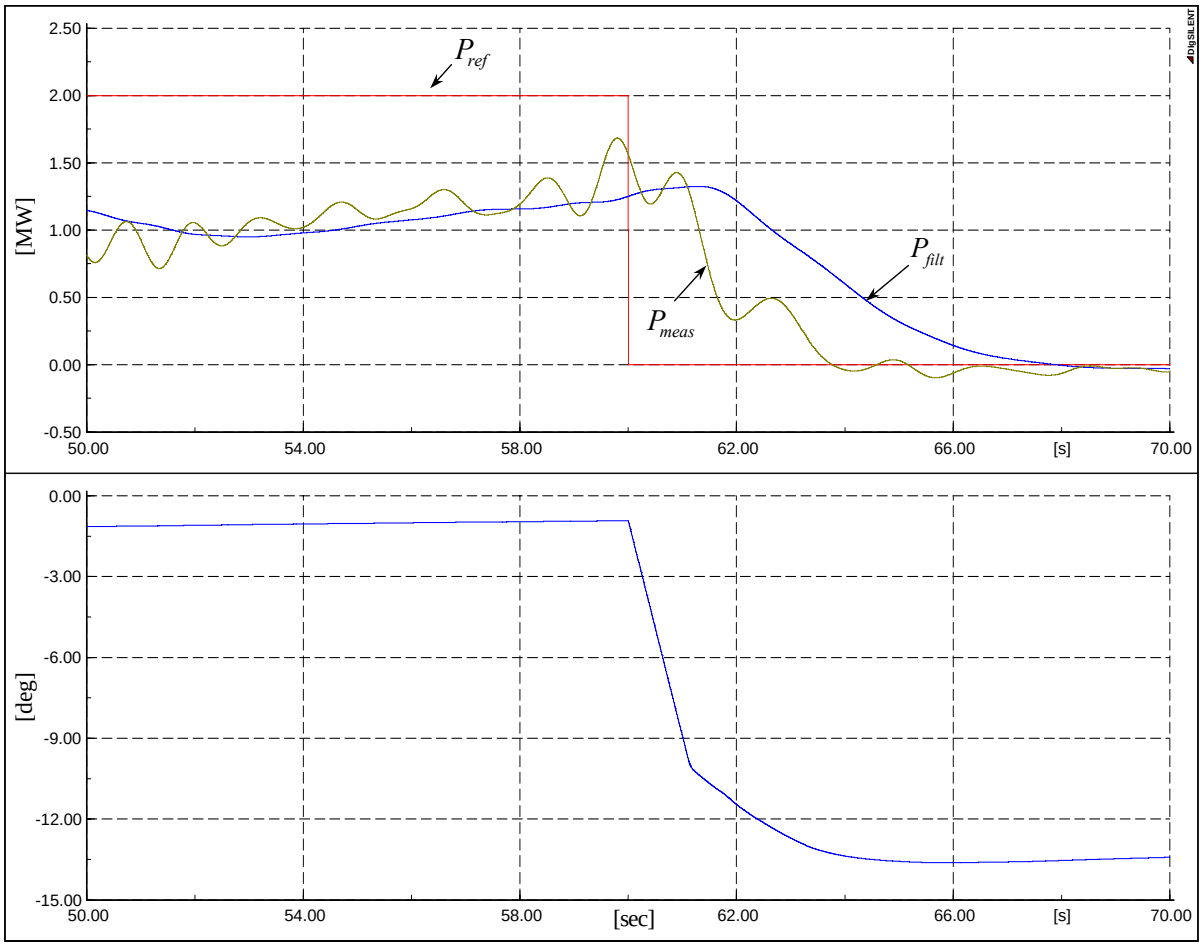

Figure 39: Detailed view of the power reference responses illustrated in Figure 38.

Figure 40 illustrates the simulation results for the reactive power control, sketched in Figure 20. The simulation case is the same as shown in Figure 38. The reactive power in MSP is controlled to zero, by switching on or off a certain number of capacitors. In the present simulation, a capacitor bank consisting of 12 steps with 0.1 MVar is used. A clock with 20 ms sampling period assures a necessary fast switch of the capacitors. With this fast sampling period, as it is seen in Figure 40, the reactive power is changed immediately by capacitor switchings as soon as the reactive power exceeds the hysteresis interval ±150 kVar. Figure 40 shows also the number of switched on capacitors during the simulation. Notice that, as expected, a step down in the active power reference implies a reduction of the reactive power demand, and as a result, the number of connected capacitors is decreased.

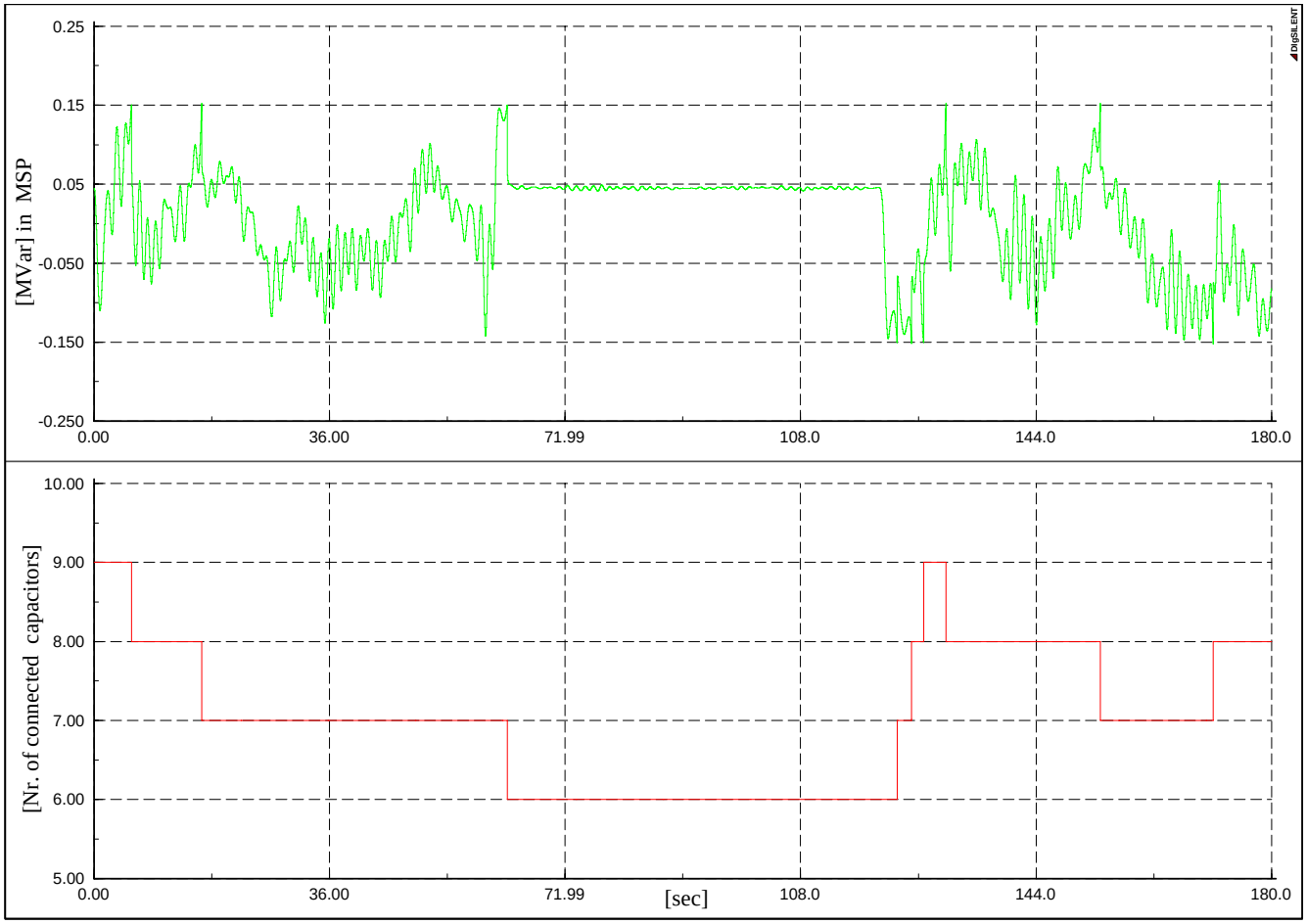

Figure 40: Reactive power control for the active stall controlled wind turbine.

The focus in the next simulations is on the wind farm controller performance in the PCC of the wind farm. Therefore the simulation results only at the wind farm level are presented. Figure 41 illustrates the performance of the wind farm power controller, when the active power demands from the grid operators is stepped down and up to different setpoints. The reactive power reference for the whole wind farm is kept to zero. The wind turbines in the wind farm are driven by different turbulent winds with 9 m/s mean speed value and 10% turbulence intensity. Figure 41 shows the estimated available power, the power demand, the power reference and the measured power in the PCC of the wind farm. In order to test the performance it is assumed that the power demand from the operators is first stepped down from 6 to 2, 1 and 0, respectively, and then stepped up vice versa.

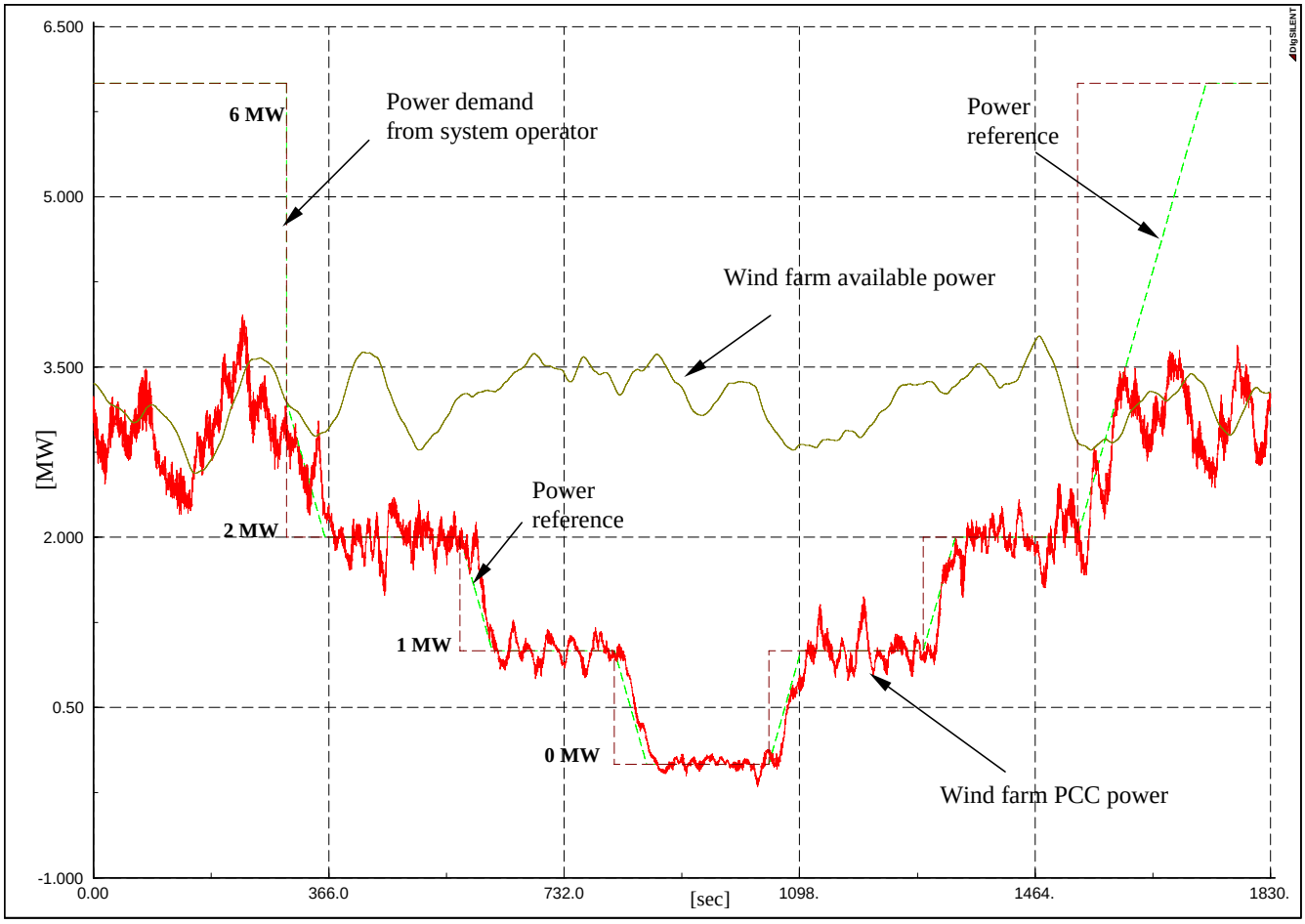

Figure 41: Wind farm response in balance control with stochastic wind speed of 9m/s and turbulence intensity of 10%.

The first and last 300 sec, the wind farm performs a normal operation and it has to produce maximum power. Notice that in this operation mode, the power reference is set to the rated power of the whole wind farm. The wind farm controller is designed in such a way that in normal operation, it allows the wind farm to produce more than the wind farm estimated available power, if this is possible. The production is thus not restricted to the estimated available power and therefore unnecessary pitch activity at each wind turbine is avoided, as it can be seen by the steady pitch angle in Figure 38. Note in Figure 41, that in the first and last 300 sec, the wind farm has the possibility to produce more than the estimated available power. At the wind turbine level this is reflected by a low pitch activity, the pitch angle being kept nearly constant to the optimal pitch value.

The simulation results show a good performance of the control system. The adjustment upwards and downwards of the wind farm production is performed with a power ramp rate limiter of about ± 1.2 MW/min. In power limitation mode the wind farm production follows properly the wind farm elaborated power reference, taking the power ramp rate limiter into account. Notice that the power fluctuations decrease at lower power references. The demand of producing 0 MW is achieved properly by the wind farm. At the wind turbine level this is reflected by a slight oscillation in the machine's speed between generator and motor modes.

Figure 42 illustrates the performance of the wind farm controller, when the reactive power demands from the grid operator is stepped up and down to different setpoints. There are two graphs: the first shows the whole sequence while the second provides a detailed view on the reactive power response at a step moment in the reactive power demand. The wind turbines are again driven by different turbulent winds with 9 m/s mean speed and 10% turbulence intensity. It is assumed that the wind farm is ordered to have maximum active power production. In order to test the performance of the reactive power wind farm controller, the reactive power demands are stepped up from 0 to 1, 2 and 3 respectively and then stepped down vice versa. Notice that the adjustments upwards and downwards of the wind farm reactive power production are performed very quickly as long as the size of capacitor bank permits that. The new reactive power reference is reached in less than 0.5 seconds. This quick performance is attractive from a grid support point of view. At a wind speed 9 m/s, each wind turbine generator produces around 1.1 MW and consumes about 0.5Mvar. This means that the whole wind farm consumes about 1.5 MVar. As each wind turbine presents a capacitor bank with 12 steps, each of 0.1 MVar, it means that for a wind speed about 9 m/s, the wind farm has a reactive power reserve of about 2 MVar. This is clearly illustrated in Figure 42, when the 3 MVar reactive power demand cannot be reached.

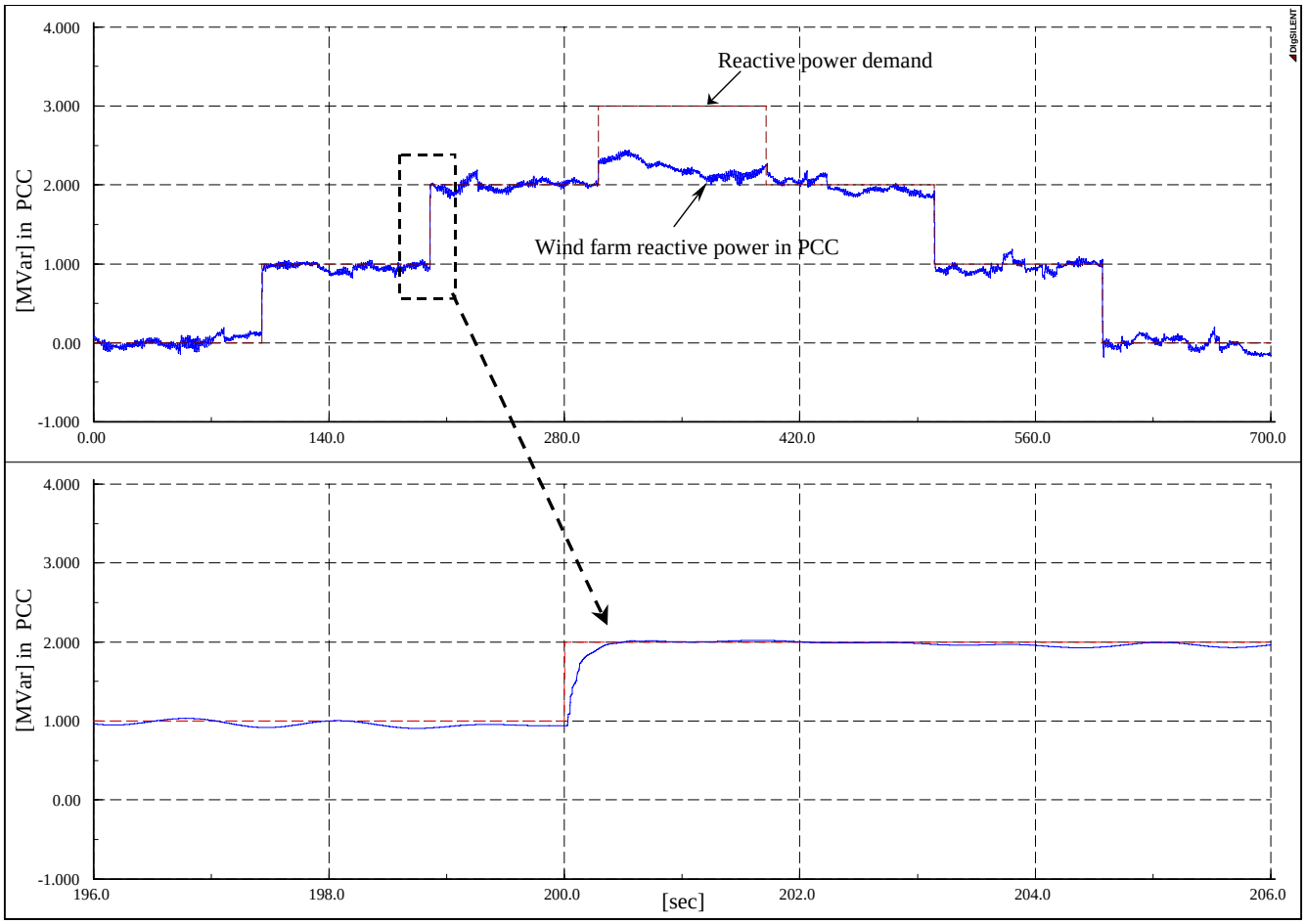

Figure 42: Reactive power response for the wind farm.

6.2 Pitch controlled double fed wind turbines with AC transmission

Figure 43 and Figure 44 show a simulation case with the doubly-fed wind farm controller. The intension of this simulation case is to illustrate how the wind farm controller is able to control the wind farm to deliver constant power in PCC. The wind farm balance power is set to 4 MW. A mean wind speed of 16 m/s has been selected, but to test the wind farm controller, an additional large drop in the wind speed of wind turbine 1 is applied as seen in Figure 43.

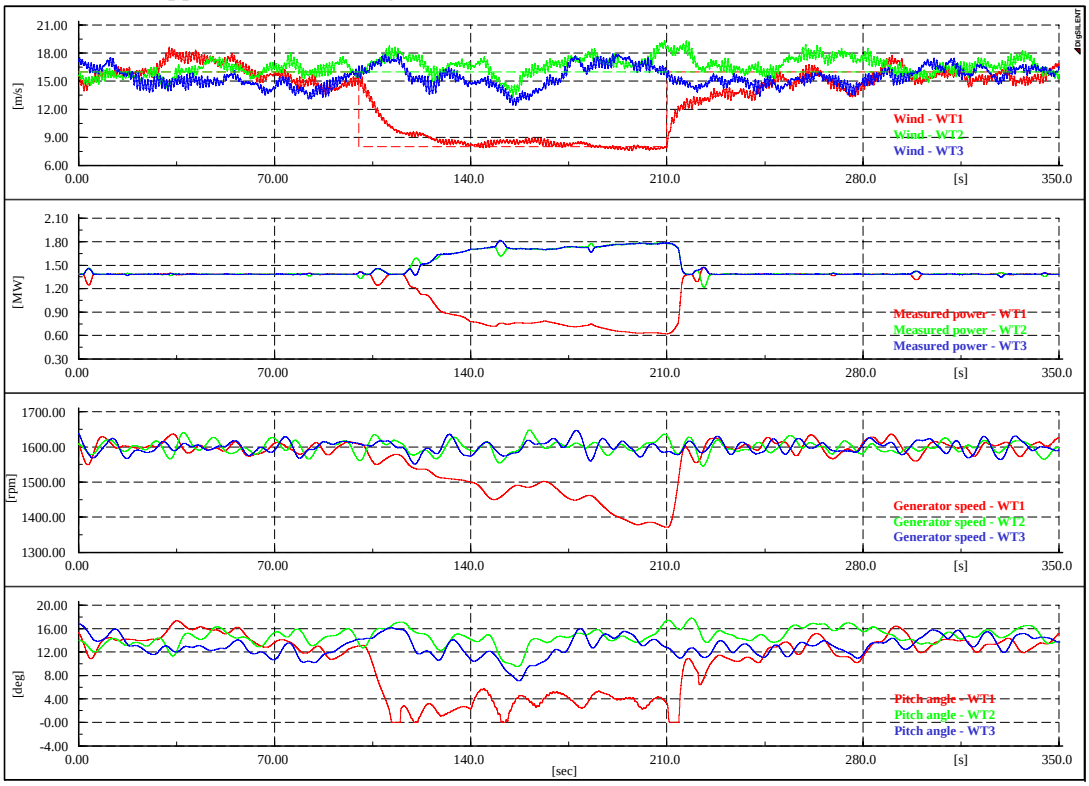

Figure 43 Wind turbines response to simulations of wind farm balance control .

Figure 44 shows available and actual power in each of the 3 wind turbines and on the wind farm. It is seen that the wind farm keeps the specified 4MW actual power very smoothly, although the power varies at the individual wind turbines. It can also be observed that the way the wind turbines distribute the power is proportional to the available power.

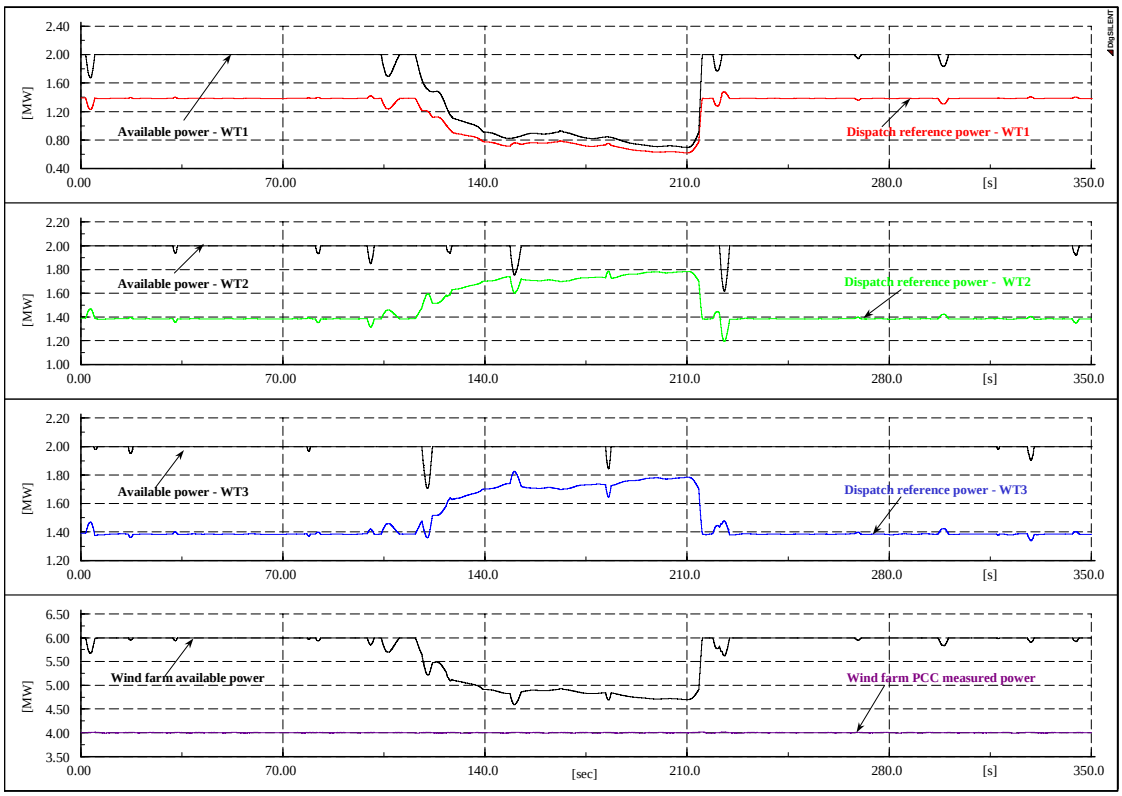

Figure 44 Actual and available power for simulations of wind farm balance control.

6.3 HVDC/VSC transmission and active/combi stall controlled wind turbines

This section shows simulations with the wind farm controller for variable speed operation with maximum power tracking. For comparison, simulations with fixed frequency are shown first.

Fixed Voltage/Frequency Operation

The instantaneous wind speed and its corresponding moving average as well as the pitch angle for each wind turbine from the wind farm are shown in Figure 45.

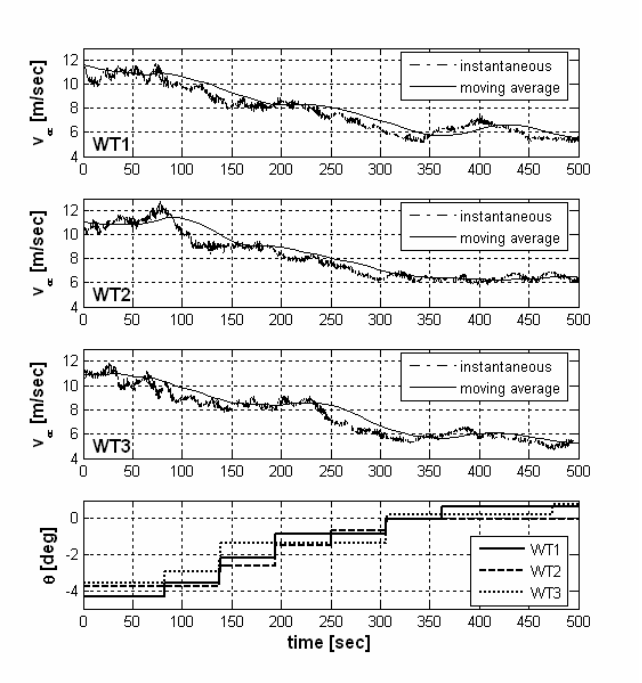

Figure 45. Wind speeds and pitch angles for each wind turbine.

It can be noticed that the pitch angle for each turbine is modified every 60 sec according with the average wind speed.

Figure 46 shows the mechanical torque and the rotor speed for the wind turbines.

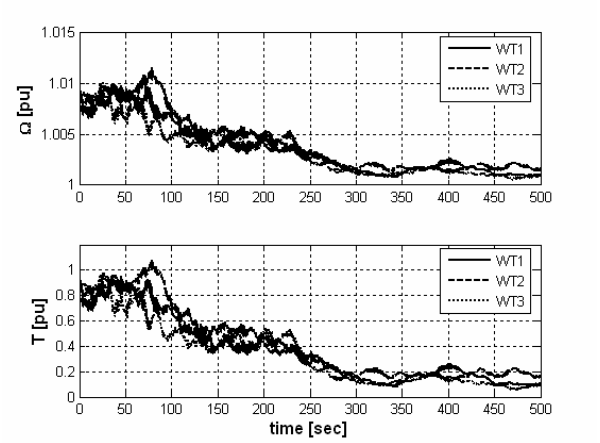

Figure 46. Mechanical torque and rotor speed for each wind turbine.

The reactive power demand for the generators is supplied by the sending end station. The active power and reactive power in the connection points of each wind turbine are shown in Figure 47.

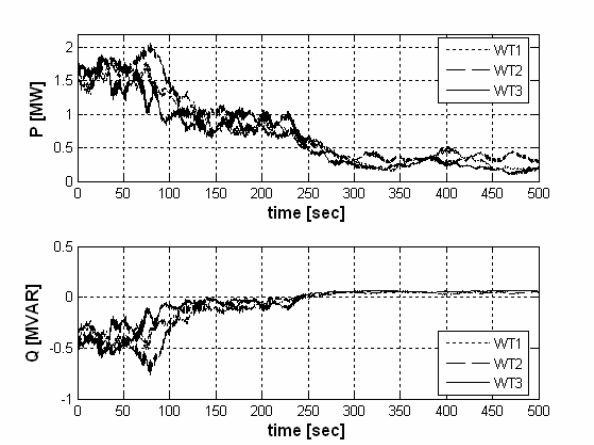

Figure 47. Active and reactive power of the wind turbines.

Finally, the voltage and frequency profiles for each station as well as the DC-link voltage are presented in Figure 48. The variations of the voltages on the bus bars are below 0.5%. The DC voltage is measured at the terminals of the Station B. The voltage variations in this case are less than ±1.5% while the controller permits a voltage drop of ±5%.

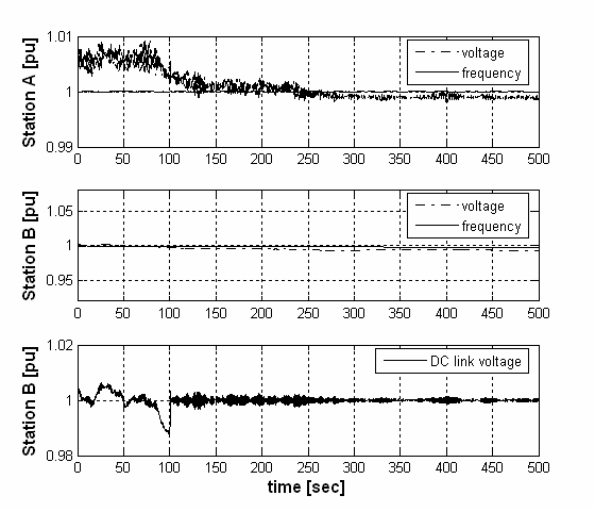

Figure 48. Voltage and frequency for the DC transmission system.

Variable Voltage/Frequency Operation

In this case it can be noticed that the pitch angle for each turbine kept constant at its optimum value all the time (Figure 49). There is short change in the pitch angle of wind turbine 2 because the output power exceeds its rated value and the pitch controller takes action in order to limit the power.

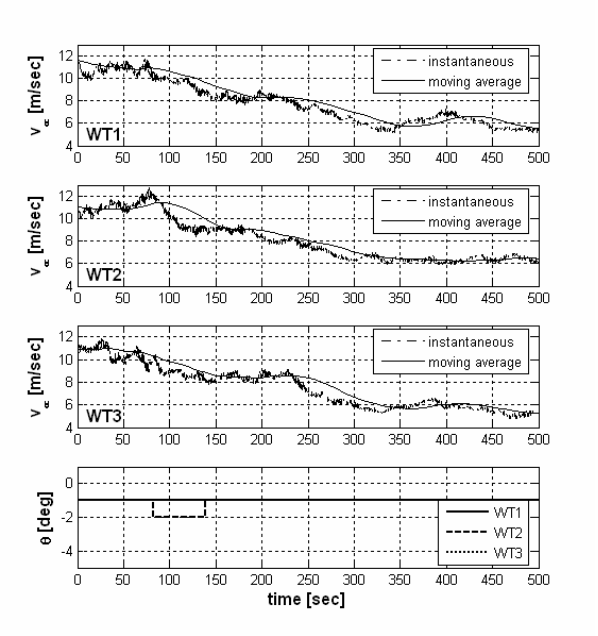

Figure 49. Wind speed and pitch angle for each wind turbine

Since the wind farm operate at the same variable frequency computed based on the maximum moving average wind speed inside the wind farm all three wind turbines have the same average rotor speed as shown in Figure 50.

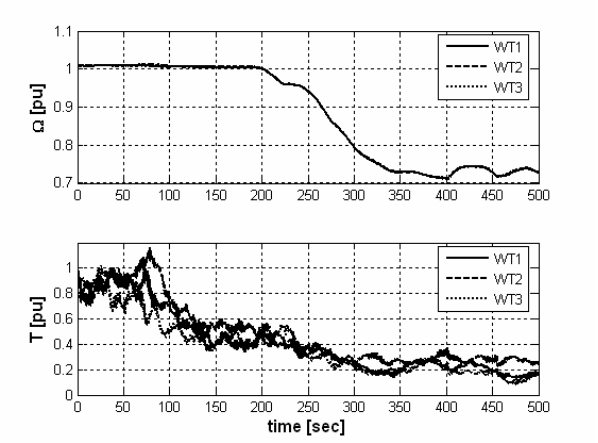

Figure 50. Mechanical torque and rotor speed for each wind turbine.

The active and reactive power time series with production sign are presented in Figure 51.

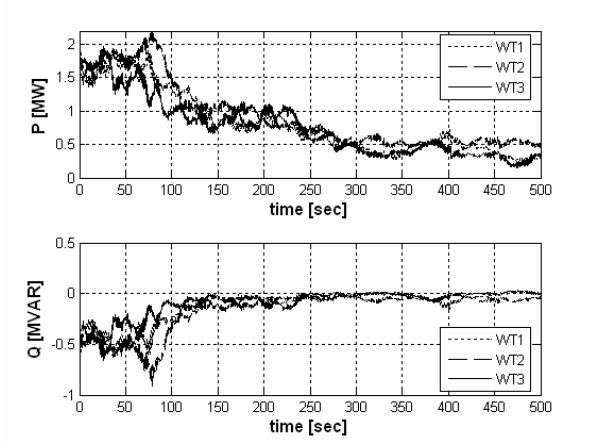

Figure 51. Active and reactive power of the wind turbines

The voltage and frequency time series for each station as well as the DC-link voltage are presented in Figure 52. The variations of the voltages on the bus bars are again below ±0.5%, while the variations for DC-link voltage are around ±1.5%.

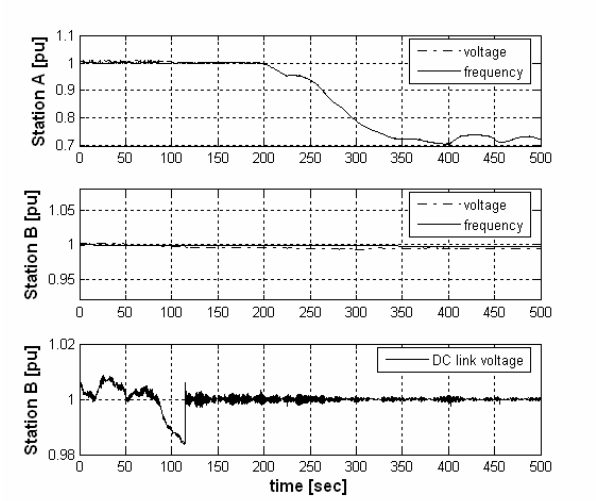

Figure 52. Voltage and frequency for the DC transmission system

7 Conclusions

The main conclusions of the work are:

- Wind speed predictions cannot improve the maximum power tracking of variable speed wind turbines. Although the speed control of the wind turbine is quite slow compared to the wind fluctuations, and therefore the rotor speed deviates from the optimal value, these deviations are relatively small. Moreover, because the Cp curve is flat on the top, small deviations in speed from the optimal causes even smaller deviations in the power from the optimal (maximum obtainable) power. Therefore, even with a perfect wind speed forecast, and if the wind turbine rotor speed would be able to follow the forecasted wind fluctuations, the power production can only be increased with

0.1 %. Since perfect forecast as well as perfect dynamic speed control is impossible, it is not likely that the power production can be increased that way.

- Simulations confirm that the two concepts used in the two large offshore wind farms in Denmark (Doubly-fed in Horns Rev and Combi stall in Nysted) can be controlled by a central wind farm controller to support power /frequency and reactive power / voltage control in the grid.
- Dynamic phase control, which is used in the Combi stall wind turbines in Nysted and can be used in similar active stall wind turbines, provides immediate response to reactive power demands. This is very useful, because the voltage can be controlled very quickly that way. The immediate response is obtained in the simulations by introducing hysteresis in the control loop. Alternatively, a low pass filter would be required, which would have slowed down the response.
- The Combi stall / active stall wind turbines can also provide a relatively fast response to changes in active power demands. Simulations with tuned, stable and fast controllers, show that a new power set point is reached fully in approximately 4 seconds. This is obtained by blade pitching.
- Variable speed wind turbines can respond immediately to changes in active as well as reactive power demands. Simulations with wind farm controller show how wind speed dips in one wind turbine can be compensated immediately by other wind turbines, which ensures a constant and very smooth power from the wind farm in the point of common coupling.

References

[1] H.A. Panofsky and J.A. Dutton. Atmospheric turbulence. John Wiley and Sons. New York 1984.

[2] H. Aa. Nielsen, H. Madsen, P. Sørensen. Ultra-short term wind speed forecasting. European Wind Energy Conference. London 2004.

[3] A.J.Wood and B.F.Wollenberg. Power generation operation and control. Second Edition. John Wiley & Sons, Inc. New York 1996.

[4] B.M.Weedy and B.J.Cory. Electric power systems. Fourth Edition. John Wiley & Sons, Ltd. Chichester 1998.

[5] S. Lindahl. Verification of governor response during normal operation. IEEE/PES Summer meeting. Chicago, USA 21-25 July 2002.

[6] Vindmøller tilsluttet net med spændinger under 100 kV. Teknisk forskrift for vindmøllers egenskaber og regulering. Elkraft System og Eltra. TF 3.2.6. November 2004.

[7] Vindmøller tilsluttet net med spændinger over 100 kV. Teknisk forskrift for vindmølleparkers egenskaber og regulering. Elkraft System og Eltra. TF 3.2.5. December 2004.

[8] L. Holdsworth, J. B. Ekanayake, N. Jenkins. Power System Frequency Response from Fixed Speed and Doubly Fed Induction Generator based Wind Turbines. Wind Energy vol. 7, p. 21-35 (2004).

[9] M. O'Malley. System Integration of wind turbines in Ireland. Proceedings of 44th IEA topical expert meeting: System integration of wind turbines. Dublin November 2004.

[10] V. Akhmatov, J. P. Kjærgaard, H. Abildgaard. Announcement of the large offshore wind farm Horns Rev B and experience from prior projects in Denmark. European Wind Energy Conference EWEA 2004. London November 2004.

[11] K. Thomsen. Operation and control of large wind turbines and wind farms - design load basis. Risø I-1967(EN). Roskilde April 2003.

[12] J. T. Petersen, "Kinematically nonlinear finite element model of a horizontal axis wind turbine," Risø National Laboratory, Roskilde, Denmark, Risø, Jul. 1990.
[13] T. J. Larsen, H. A. Madsen, K. Thomsen. Active Load Reduction Using Individual Pitch, Based on Local Blade Flow Measurements. Wind Energy vol. 8 p. 67-80 (2005).
[14] M. H. Hansen (editor), A. Hansen, T. J. Larsen, S. Øye, P. Sørensen and P. Fuglsang. Control design for a pitch-regulated, variable speed wind turbine. Risø R-1500. Roskilde January 2005.
[15] L. J. Fingersh, P. W. Carlin. Results from the NREL Variable-Speed Test Bed. Proceedings of the 17th ASME Wind Energy Symposium, Reno, NV, 1998, pp. 233-237.
[16] K. E. Johnson, L. J. Fingersh, M. J. Balas, L. Y. Pao. Methods for increasing region 2 power capture on a variable speed HAWT. 23rd ASME Wind Energy Symposium, Reno, Nevada. January 2004.
[17] J.R.Kristoffersen, P.Christiansen. Horns Rev offshore wind farm: its main controller and remote control system. Wind Engineering Volume 27, No 5 2003, p 351-360.
[18] P. Sørensen, A. D. Hansen, P. A. C. Rosas. Wind models for simulation of power fluctuations from wind farms. J. Wind Eng. Ind. Aerodyn. (2002) (no.90) , 1381-1402.
[19] P. Sørensen, A.D. Hansen, L. Janosi, J. Bech, B. Bak-Jensen. Simulation of Interaction between wind farm and power system, Risø-R-1281 (EN), 2001.
[20] S. Øye. "Dynamic stall - simulated as time lag of separation", In *Proceedings of the 4th IEA Symposium on the Aerodynamics of Wind Turbines*, McAnulty, K. F (Ed.), 1991, Rome, Italy.
[21] C. Jauch, A.D. Hansen, P. Sørensen, F. Blaabjerg. Simulation model of an active-stall fixed-speed wind turbine controller. Wind Engineering, 2004, Vol.28, No.2, pp. 177- 195.
[22] P. Sørensen, F. Iov, F. Blaabjerg, J. Skaarup. Test and simulation of dynamic phase compensation from Mita- Teknik A/S, Risø-R-1438 (EN), 2004.
[23] Hansen, A.D.; Sørensen, P.; Iov, F.; Blaabjerg, F., Centralised power control of wind farm with doubly fed induction generators. Renewable Energy (Article in press).
[24] F.Schettler, H. Huang, N. Christl – *HVDC transmission systems using voltage sourced converters – Design and applications*, IEEE Proceed. on Power Eng. Soc. General Meeting, 2000, vol.2, pp. 715-720.
[25] M.P. Bahrman, J.G. Johansson, B.A. Nielsen – *Voltage source converter transmission technologies – the right fit for the application*, IEEE Proceed. on Power Eng. Soc. General Meeting, 2003, vol.3, pp.1840-1847.
[26] A-K Skytt, P.Holmberg, L-E Juhlin – *HVDC Light for connection of wind farms*, Proceed. on 2nd International WorkShop on Transmission Networks for Offshore Wind Farms, Royal Institute of Technology Stockholm, Sweden, March 29-30, 2001.
[27] K.H. Søbrink, P.L. Sørensen, et all – *DC Feeder for connection of a wind farm*, Proceeed. On Cigre Symposium, Kuala Lumpur, Malaysia, September 1999.
[28] DIgSILENT Technical Documentation – *PWM-Converter. Model Description*, doc. TR-003, build 223, September 4 2003, DIgSILENT GmbH Germany.
[29] R. H. Lasseter – *Microgrids*, IEEE Power Engineering Society Winter Meeting, 2002, Vol. 1, 27-31 Jan. 2002, pp. 305 – 308.
[30] P. Karlsson – *DC Distributed Power Systems. Analysis, Design and Control for a Renewable Energy system*, PhD Dissertation, Lund University, Sweden, 2002, ISBN 91-88934-25-X.
[31] F. Iov, P. Soerensen, A. Hansen, F. Blaabjerg Grid connection of active stall wind farms using a VSC based DC transmission system, in Proc. of European Power Electronics Conference EPE 2005, 11-14 September, Dresden, Germany, 10 pp., ISBN 90-75815-08-5

[32] F. Iov, P. Soerensen, A. Hansen, F. Blaabjerg - Variable Frequency operation of Active Stall Wind farms using a DC Connection to Grid, in Proc. of IASTED - Energy and Power System Conference EPS 2005, 18-21 April 2005, Krabi, Thailand, 8 pp., ISBN: 0-88986-494-2

[33] F. Iov, P. Soerensen, A. Hansen, F. Blaabjerg - Modelling and Control of VSC based DC Connection for Active Stall Wind Farms to Grid, in Proc. of IEE - International Power Electronics Conference IPEC 2005, 4-8 April, Niigata, Japan, ISBN 4-88686-065-6

Mission

To promote an innovative and environmentally sustainable technological development within the areas of energy, industrial technology and bioproduction through research, innovation and advisory services.

Vision

Risø's research **shall extend the boundaries** for the understanding of nature's processes and interactions right down to the molecular nanoscale.

The results obtained shall **set new trends** for the development of sustainable technologies within the fields of energy, industrial technology and biotechnology.

The efforts made **shall benefit** Danish society and lead to the development of new multi-billion industries.